AD_____

Award Number: DAMD17-99-1-9129

TITLE: Rational Design of Human Prolactin Receptor Antagonists for Breast Cancer Therapy

PRINCIPAL INVESTIGATOR: Wen Y. Chen, Ph.D.

CONTRACTING ORGANIZATION: Clemson University
Clemson, SC 29634-5702

REPORT DATE: October 2004

TYPE OF REPORT: Final Addendum

PREPARED FOR: U.S. Army Medical Research and Materiel Command
Fort Detrick, Maryland 21702-5012

DISTRIBUTION STATEMENT: Approved for Public Release;
Distribution Unlimited

REPORT DOCUMENTATION PAGE

Form Approved
OMB No. 074-0188

1. AGENCY USE ONLY (Leave blank)	2. REPORT DATE	3. REPORT TYPE AND DATES COVERED
	October 2004	Final Addendum (15 Sep 2003 - 14 Sep 2004)

4. TITLE AND SUBTITLE
Rational Design of Human Prolactin Receptor Antagonists for Breast Cancer Therapy

5. FUNDING NUMBERS
DAMD17-99-1-9129

6. AUTHOR(S)
Wen Y. Chen, Ph.D.

7. PERFORMING ORGANIZATION NAME(S) AND ADDRESS(ES)
Clemson University
Clemson, SC 29634-5702

E-Mail: wenc@clemson.edu

8. PERFORMING ORGANIZATION REPORT NUMBER

9. SPONSORING / MONITORING AGENCY NAME(S) AND ADDRESS(ES)
U.S. Army Medical Research and Materiel Command
Fort Detrick, Maryland 21702-5012

10. SPONSORING / MONITORING AGENCY REPORT NUMBER

11. SUPPLEMENTARY NOTES
Original contains color plates: ALL DTIC reproductions will be in black and white

12a. DISTRIBUTION / AVAILABILITY STATEMENT
Approved for Public Release; Distribution Unlimited

12b. DISTRIBUTION CODE

13. ABSTRACT (Maximum 200 Words)

There were two specific tasks listed in the proposal i.e. development of hPRL-G129R as a PRL receptor antagonist and development of PRL BP as PRL sequester as potential breast cancer therapeutics. The conclusions from this project are that we have demonstrated that hPRL-G129R has promise to be used as a breast cancer therapeutic, but not hPRL-BP. We have found that hPRL-G129R is able to inhibit breast cancer cell proliferation via the induction of apoptosis. We further presented evidence that shows the mechanism of hPRL-G129R induced breast cancer cell apoptosis is through the regulation of Bcl-2/Bax gene expression. Data obtained from mouse breast cancer model also support the notion that the inhibition of PRL activity in breast cancer will inhibit its growth. In addition, we explored the possibility of using hPRL-G129R as a targeting molecule by creating fusion molecules such as G129R-IL-2) and G129R-endostatin. During past year, we have published 2 manuscripts directly related to this subject. In summary, we have further demonstrated that hPRL-G129R is a true PRL receptor antagonist. Its anti-breast tumor effects were confirmed using both in vitro and in vivo assays.

14. SUBJECT TERMS
Breast Cancer

15. NUMBER OF PAGES
21

16. PRICE CODE

17. SECURITY CLASSIFICATION OF REPORT	18. SECURITY CLASSIFICATION OF THIS PAGE	19. SECURITY CLASSIFICATION OF ABSTRACT	20. LIMITATION OF ABSTRACT
Unclassified	Unclassified	Unclassified	Unlimited

Table of Contents

Key Research Accomplishment

During the past year after we submitted final report related to this grant, we have published 2 manuscripts and 4 national meeting presentations (abstracts) directly related to this research. In summary, we have demonstrated that hPRL-G129R is a true PRL receptor antagonist. Its anti-breast tumor effects were confirmed using both in vitro and in vivo assays. In addition, we have demonstrated that hPRL-G129R may be used as a targeting vehicle to produce breast cancer specific therapeutics.

Reportable Outcomes

Two manuscripts:

1. Beck MT, Chen, NY, Franek K and Chen WY. Prolactin Antagonist Endostatin Fusion Protein as A Targeted Dual Functional Therapeutic Agent for Breast Cancer. Cancer Res., 63:3598-3604, 2003.
2. Peirce S and Chen WY. Human prolactin and its antagonist, hPRL-G129R, regulate *bax* and *bcl-2* gene expression in human breast cancer cells and transgenic mice. Oncogene 23:1248–1255, 2004.

Four Abstracts (National Meeting presentations).

1. Langenheim JF and Chen WY. Development of A Prolactin Receptor-Targeting Fusion Toxin Using A Prolactin Receptor Antagonist and a Recombinant Form of Pseudomonas Exotoxin A. AACR 2004.
2. Park JP and Chen WY. Development of A Vascular Endothelial Growth Factor Receptor Antagonist. AACR 2004
3. Jacquemart IL and Chen WY Genetic Profiling to Identify Alterations in Gene Expression in the Mammary Gland of MMTV/neu Transgenic Mice that are Responsible for the Suppression of Her2/neu-initiated Breast Tumors. AACR 2004
4. Tomblyn S and Chen WY. Microarray Profiling to Identify the Genes Responsible for Prolactin (PRL) or a Prolactin Antagonist (G129R) Induced Morphological Alterations in the Mammary Glands of Transgenic Mice. Endo. 2004.

There is no personnel covered under this grant during the 12 month period of the extension.

Conclusions:

Through the DoD funding, we have confirmed that that hPRL-G129R acted as a true hPRL receptor antagonist in human breast cancer cells both in vitro and in vivo. We have also made considerable progress in designing hPRL-G129R based targeting therapeutics for breast cancer. This DoD idea award has provided PI valuable resources to advance his career in his critical time as a junior faculty member. This award also helped several graduate students to complete their training in the field of breast cancer research. The data generated through this award has resulted in multiple publications; part of the data has been used to generate new proposals for potential future funding. Again, the PI would like to extent his sincere thanks to DoD for this award.

Appendices

Two manuscripts

Oncogene (2004) 23, 1248–1255

www.nature.com/onc

Human prolactin and its antagonist, hPRL-G129R, regulate *bax* and *bcl-2* gene expression in human breast cancer cells and transgenic mice

Susan K Peirce[1] and Wen Y Chen*[,2,3]

[1]*Department of Genetics and Biochemistry, Clemson University, Clemson, SC 29630, USA;* [2]*Department of Biological Sciences, Clemson University, Clemson, SC 29630, USA;* [3]*Oncology Research Institute, Greenville Hospital System, 900 West Faris Road, Greenville, SC 29605, USA*

To gain insight into the molecular mechanisms involved in human prolactin receptor antagonist (hPRL-G129R)-induced apoptosis, we used real-time reverse transcription–polymerase chain reaction to measure *bax* and *bcl-2* gene expression in 11 human breast cancer cell lines following treatment with hPRL and hPRL-G129R. We also measured *bax* and *bcl-2* gene expression in the mammary glands of transgenic mice expressing hPRL or hPRL-G129R. A time-course study of hPRL and antagonist treatment in T-47D cells indicated changing *bax*/*bcl-2* mRNA ratios beginning at 24 h. We found that *bax*/*bcl-2* mRNA ratios were significantly elevated in seven of the 11 hPRL-G129R-treated cell lines, as well as in the hPRL-G129R transgenic mice. To confirm these results, Bax and Bcl-2 proteins were analysed by Western blot methods in mammary gland tissue homogenates of transgenic mice. Bax/Bcl-2 ratios were highest in the 6-month group of hPRL-G129R transgenics, and lowest in the 6-month group of hPRL transgenics. We expanded our findings by examining the release of a downstream Bax-induced protein, cytochrome *c*, a hallmark protein of apoptosis, in transgenic mice. Again, cytochrome *c* levels were highest in the 6-month hPRL-G129R transgenic group. Thus, hPRL-G129R-induced breast cancer cell and/or mammary gland apoptosis is mediated, at least in part, through the regulation of Bax and Bcl-2 gene expression.

Oncogene (2004) **23,** 1248–1255. doi:10.1038/sj.onc.1207245
Published online 1 December 2003

Keywords: prolactin antagonist; bax; bcl-2; cytochrome *c*; breast cancer; apoptosis

Introduction

Prolactin (PRL) is a member of a group of polypeptide hormones that includes growth hormone and placental lactogen. Synthesized primarily by lactotropes in the anterior pituitary, PRL is critically involved in normal mammary gland development (Nagasawa *et al.*, 1985; Clevenger *et al.*, 1995; Vonderhaar, 1998; Blackwell and Hammond, 1999). In addition to its role as an endocrine hormone, human PRL (hPRL) is also produced by the breast epithelium as an autocrine/paracrine growth factor, and as such functions as a cytokine (Clevenger *et al.*, 1995, 2003; Ginsburg and Vonderhaar, 1995; Ben-Jonathan *et al.*, 2002). The finding of the extrapituitary role of hPRL links hPRL to human breast cancer (Vonderhaar, 1999) and includes evidence such as (a) the detection of biologically active hPRL in human breast cancer cells and tumors (Clevenger *et al.*, 1995; Ginsburg and Vonderhaar, 1995; Bhatavdekar *et al.*, 2000); (b) the finding of increased levels of hPRL receptor (PRLR) levels in human breast cancer cells over normal breast epithelial cells (Binart *et al.*, 2000); (c) the finding that transgenic mice overexpressing hPRL have a higher breast cancer rate (Wennbo *et al.*, 1997); (d) the recent observation that hPRL stimulates angiogenesis (Corbacho *et al.*, 2002); and (e) the finding that the hPRL antagonist hPRL-G129R slows the growth rate of human breast cancer cells *in vitro* and in xenografts of nude mice (Chen *et al.*, 1999, 2002). Taken together, these findings lend support to the mitogenic importance of hPRL in breast cancer development and progression, and suggest that its antagonist could have a potential in treating human breast cancer.

The elimination of tumors by the induction of apoptosis, or programmed cell death, is the most common mechanism of cancer therapeutics (Zhang *et al.*, 2000). One of the first regulators of apoptosis to be identified was Bcl-2, which is now known to be an antiapoptotic member of one of three subfamilies of related proteins, all of which share at least one Bcl-2 homology (BH) domain (Adams and Cory, 1998; Cory and Adams, 2002). It is encoded by *bcl-2*, a human proto-oncogene (Korsmeyer, 1999), and suppresses apoptosis by blocking the release of cytochrome *c* (a heme protein required for cellular respiration) from the mitochondria, thus preventing the activation of caspases, a group of cysteine proteases that carry out the process of cell death (Yin *et al.*, 1994; Kumar *et al.*, 2000). Bcl-2 remains associated with the outer mitochondrial membrane, maintaining its integrity. In response to damage or stress signals, Bax monomers are translocated from the cytosol, oligomerize, and induce permeabilization of the mitochondrial mem-

*Correspondence: WY Chen, Oncology Research Institute, Greenville Hospital System, 900 West Faris Road, Greenville, SC 29605, USA; E-mail: wchen@ghs.org
Received 12 August 2003; revised 25 September 2003; accepted 25 September 2003

brane, leading to the release of proapoptotic proteins and activation of several key caspases, most notably caspase 9. This permeabilization is thought to function as the 'apoptotic checkpoint' (Debatin *et al.*, 2002). In human mammary tissue, Bcl-2 and Bax, its proapoptotic homolog, are constitutively expressed to tightly regulate apoptosis during normal developmental processes (Yin *et al.*, 1994; Binder *et al.*, 1996; Adams and Cory, 1998; Kumar *et al.*, 2000). Breast malignancy requires the upregulation of *bcl-2* gene expression, ultimately resulting in the inhibition of apoptosis (Green and Beere, 1999; Krajewski *et al.*, 1999). Studies using Nb2 cells, a rat lymphoma hPRL-dependent cell line, have demonstrated *bcl-2* upregulation and *bax* downregulation following treatment with hPRL (Krumenacker *et al.*, 1998; Schorr *et al.*, 1999).

In our previous studies, we reported that hPRL and hPRL-G129R regulate Bcl-2 gene expression in multiple human breast cancer cells (Beck *et al.*, 2002). In this work, we extended that study to include the measurement of *bax* gene expression and determination of the *bax/bcl-2* mRNA ratios in 11 human breast cancer cell lines, following treatment with the hPRL antagonist hPRL-G129R. A time-course study of *bax* and *bcl-2* levels in T-47D cells following hPRL and antagonist treatments was first conducted. We also quantified *bax* and *bcl-2* expression in hPRL or hPRL-G129R transgenic mice of three age groups. We confirmed our findings linking increased *bax* expression to hPRL-G129R exposure at the protein level by Western blot, and by detection of cytochrome *c* release.

Results

Bax mRNA levels and bax/bcl-2 *ratios are increased in response to hPRL-G129R treatment in a majority of human breast cancer cell lines examined*

To determine the time course of the response of T-47D cells to treatments, cells were treated with either 500 ng/ml of hPRL or hPRL-G129R. The mRNA levels of *bax* and *bcl-2* levels were measured using real-time reverse transcription–polymerase chain reaction (RT–PCR) at five time points: 2, 6, 24, 48 and 72 h. Levels of *bax* and *bcl-2* were normalized to levels in the untreated samples, and results are presented as the ratio of treated to untreated values for each time point. The maximum response of *bax* to hPRL-G129R treatment was observed after 48 h of treatment (Figure 1a). *bax* levels at 24, 48 and 72 h were all statistically different from those of the untreated cells. Figure 1b, representing the time course of *bcl-2* response to hPRL and hPRL-G129R treatments, indicated that the upregulation of *bcl-2* by hPRL and downregulation by hPRL-G129R were most pronounced by 48 h. The reduction of *bcl-2* in response to hPRL-G129R treatment was more rapid than the increase in *bcl-2* levels in response to hPRL treatment. When the mean *bax/bcl-2* ratios for the hPRL and hPRL-G129R treatments were compared (Figure 1c), it is apparent that hPRL-G129R increased,

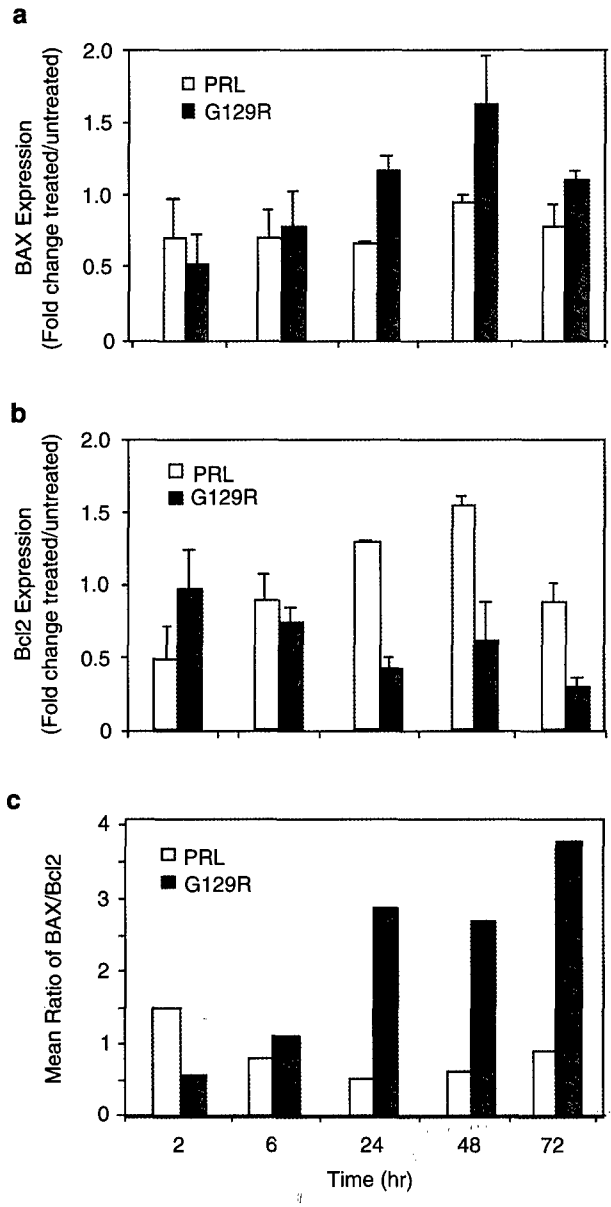

Figure 1 Time-course study of Bax and Bcl-2 mRNA levels in response to hPRL or hPRL-G129R treatment in T-47D cells, as measured by real-time RT–PCR at five different time points. Cells were treated with 500 ng/ml of hPRL or hPRL-G129R in RPMI media containing 2% CSS, and total RNA was extracted after 2, 6, 24, 48 and 72 h. Panel a, Bax mRNA levels; panel b, Bcl-2 mRNA levels; and panel c, ratios of Bax/Bcl-2 mRNA levels calculated from the mean value of each data point as fold change from the untreated controls

whereas hPRL decreased the ratio of *bax/bcl-2*. From these results, the 48 h treatment was chosen as the time point for subsequent real-time RT–PCR analyses in multiple cell lines.

As summarized in Figure 2 and Table 1, *bax* levels were significantly upregulated in response to hPRL-G129R treatment in five of the 11 cell lines (Figure 2a), with smaller increases in three cell lines. In a previous study (Beck *et al.*, 2002), we measured *bcl-2* levels in response to hPRL and hPRL-G129R treatments in these

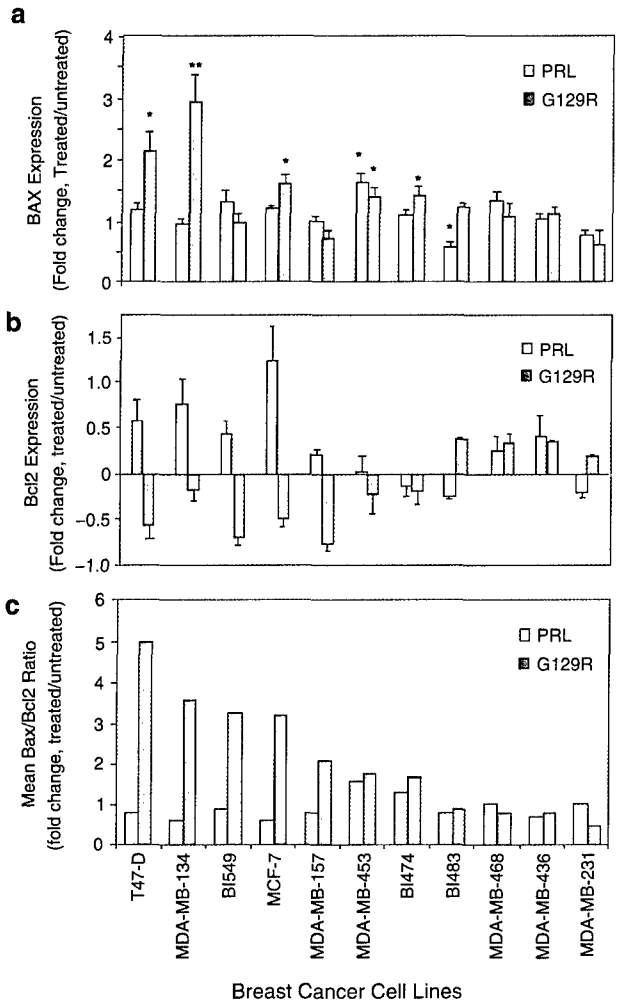

Figure 2 Bax and Bcl-2 gene expression in response to hPRL and hPRL-G129R treatment in 11 human breast cancer cell lines, as measured by real-time RT–PCR. Cells were treated with 500 ng/ml of hPRL or hPRL-G129R in RPMI media containing 2% CSS for 48 h. Panel a, Bax mRNA levels; panel b, Bcl-2 mRNA levels; and panel c, Bax/Bcl-2 mRNA ratios from real-time RT–PCR data calculated from the mean value of each cell line as fold change compared to the untreated controls. The asterisks indicate the level of significant difference from that of control (ratio of 1). A ratio of 1 would indicate no change. A single asterisk indicates a significant difference (95%), and two asterisks indicate a highly significant difference (99%)

same cell lines (Figure 2b). In the present study, we found that increases in *bax* levels in response to hPRL-G129R treatment corresponded to levels of increase in *bcl-2* in response to hPRL treatment. Presented as the mean ratio of *bax/bcl-2* (Figure 2c), the *bax/bcl-2* ratios for hPRL-G129R treatment indicated a major increase in seven of the 11 cell lines. In an earlier study (Peirce and Chen, 2001), we reported PRL receptor (PRLR) levels in these same cell lines. Here, the cell lines with the higher levels of PRLR (T-47D, BT-134, MDA-MB-453, MCF-7, BT-474) were the most responsive to both hPRL and hPRL-G129R treatments, with the two cell lines having the highest PRLR levels (T-47D and BT-134) showing the largest *bax/bcl-2* ratios (Figure 2c).

Bax and Bcl-2 mRNA levels in mammary gland tissue homogenates from MT-hPRL and MT-hPRL-G129R transgenic mice

The transgenes are regulated by the metallothionine promoter (MT) and are, therefore, constitutively expressed in a majority of tissues including the mammary gland. The transgenes are continually expressed throughout the lifetime of the animals studied (data not shown). The levels of hPRL and hPRL-G129R expression in the serum of these animals ranged between 5 and 10 ng/ml, as measured by a ^{125}I immunoradiometric serum assay, Coat-A-Count PRL IRMA (Diagnostic Products Corporation, LA, CA, USA). We did not observe any significant alteration in the ability of the PRL or G129R transgenic mice to reproduce, since both males and females of these mice are fertile. This may be due to the fact that the transgene expression levels were relatively low. Total RNA isolated from the mammary glands of hPRL or hPRL-G129R transgenic mice (4–7 mice per group; 3, 6–7 and 9–12 months of age) was analysed for levels of *bax* and *bcl-2*. Nontransgenic littermates were used as the controls. Data were presented as the ratio of gene expression levels of the transgenic mice to those of the nontransgenic littermates. Thus, a ratio of 1 indicates that there is no difference in gene expression between the transgenic and its nontransgenic littermate. Within the 3- and 6-month age groups, levels of Bax mRNA were not statistically different between hPRL and hPRL-G129R transgenic mice (Figures 3a). However, by 9 months, levels of *bax* were significantly upregulated in hPRL-G129R transgenics ($P<0.001$). Levels of Bcl-*2* mRNA showed a response at an earlier age. By 6 months, levels of Bcl-2 mRNA were highly upregulated in the hPRL group of transgenics ($P<0.01$). However, this difference diminished with increasing age of the mice; within the 9–12-month age groups, *bcl-2* levels were not significantly different between hPRL and hPRL-G129R transgenic mice. *bax/bcl-2* ratios were also compared for each age group (Figure 3b). At 3 months, there was little difference between the hPRL and hPRL-G129R transgenic mice. However, by 6–7 months, the *bax/bcl-2* ratio was 0.214 for the hPRL transgenics (largely due to upregulation of *bcl-2*) as compared to their nontransgenic littermates, and 2.43 for the hPRL-G129R transgenics (largely due to upregulation of *bax*), a 11-fold difference in *bax/bcl-2* ratios between hPRL and hPRL-G129R transgenic mice. By 9–12 months, the difference between *bax/bcl-2* ratios had diminished somewhat, to a five-fold increase in the *bax/bcl-2* ratio of the hPRL-G129R transgenics over the hPRL transgenics.

Bax, Bcl-2 and cytochrome c *protein levels in the mammary gland tissue of MT-hPRL and MT-hPRL-G129R transgenic mice*

Tissue homogenates from the mammary gland of the transgenic mice and their nontransgenic littermates for

Table 1 Summary of Bax and Bcl-2 mRNA expression in response to hPRL or hPRL-G129R treatment in 11 human breast cancer cell lines, ±s.e.

	Bax/control		*Bcl-2/control*		*Bax/bcl-2*	
Cell lines	*PRL*	*G129R*	*PRL*	*G129R*	*PRL*	*G129R*
T-47D	1.2±0.1	2.1±0.3	1.6±0.3	0.4±0.2	0.8	5.0
MDA-MB-134	1.0±0.1	2.1±0.5	1.8±0.3	0.8±0.1	0.6	3.6
MB-549	1.3±0.2	1.0±0.1	1.5±0.1	0.3±0.1	0.9	3.3
MCF-7	1.2±0.02	1.6±0.2	2.3±0.2	0.5±0.1	0.6	3.2
MDA-MB-157	1.0±0.1	0.7±0.2	1.2±0.1	0.3±0.1	0.8	2.1
MDA-MB-453	1.6±0.2	1.4±0.2	1.0±0.2	0.2	1.6	1.8
BT-474	1.1±0.1	1.4±0.1	0.9±0.1	0.8±0.2	1.3	1.7
BT-483	0.6±0.1	1.2±0.1	0.8	1.4	0.8	0.9
MDA-MB-468	1.3±0.2	1.1±0.2	1.3±0.2	1.3±0.1	1.0	0.8
MDA-MB-436	1.0±0.1	1.1±0.1	1.4±0.3	1.4	0.7	0.8
MDA-MB-231	0.8±0.1	0.6±0.2	0.8±0.1	1.2	1.0	0.5

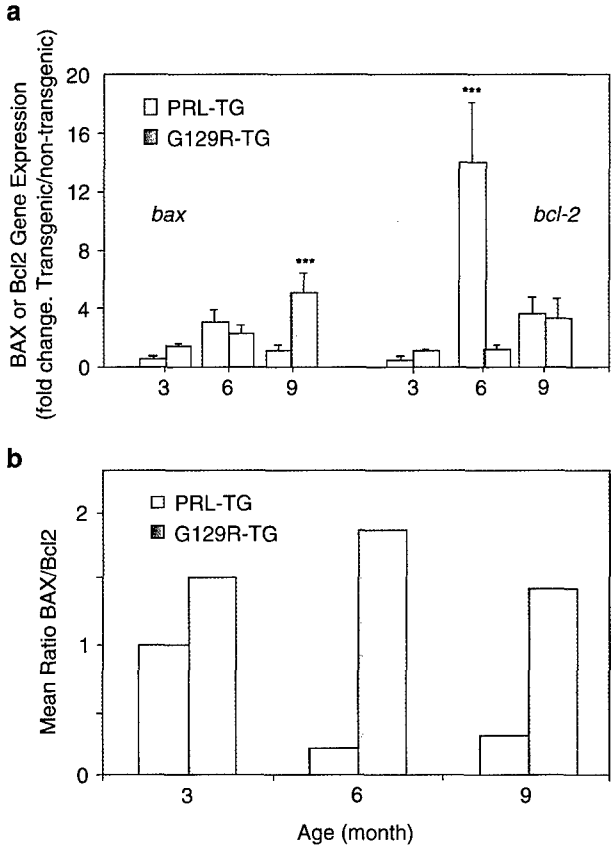

Figure 3 Bax and Bcl-2 mRNA levels in mammary gland tissues of hPRL and hPRL-G129R transgenic mice of three age groups. Bax and Bcl-2 expression levels were quantified using real-time RT–PCR, and were normalized to 18s rRNA levels. Panel a, Bax (left) and bcl-2 (right) mRNA levels in hPRL and hPRL-G129R transgenics, relative to nontransgenic littermates; and panel b, comparison of fold change of *bax/bcl-2* ratios in hPRL and hPRL-G129R transgenics adjusted to levels of nontransgenic littermates

all the three age groups were analysed for levels of Bax, Bcl-2 and cytochrome *c* proteins (Figure 4a–c). At 3 months, the levels of Bax and Bcl-2 were similar between the two groups of transgenics, although the hPRL-G129R transgenics were already expressing slightly more Bax at the protein level (Figure 4a). By 6 months, the hPRL-G129R transgenics were expressing considerably more Bax protein than the corresponding hPRL transgenics (Figure 4b). At 9 months, both transgenic groups were producing high levels of Bax (Figure 4c). When these expression levels were quantified from densitometric scans and the Bax/Bcl-2 ratios were calculated using the levels of the nontransgenic littermates as the baseline (Figure 4 inset), statistically significant differences were seen between the 6-month groups, with the hPRL-G129R transgenics expressing proportionally much higher levels of Bax. All samples were normalized to levels of α-tubulin, as quantified by densitometric scanning.

Age-matched changes in Bax and Bcl-2 levels between the two groups of transgenics were paralleled by changes in cytochrome *c* (Figure 4). At 3 months, there is a low level of cytochrome *c* expression in the hPRL-G129R group, not seen in the hPRL transgenics or the litter-matched nontransgenic animals. At 6 months, this level of cytochrome *c* expression had markedly increased in the hPRL-G129R transgenic animals. However, by 9 months, both the hPRL-G129R and the hPRL transgenic animals expressed high levels of cytochrome *c*, relative to their nontransgenic littermates. Similar results were found using human breast cancer cells (T-47D and MB-453) following treatment with hPRL-G129R. Cytosolic cytochrome *c* levels showed a dose- and time-dependent response to hPRL-G129R treatment (data not shown).

Discussion

In our previous studies, it was shown that the PRL receptor antagonist hPRL-G129R is able to inhibit human breast cancer cell proliferation through the induction of apoptosis (Chen *et al.*, 1999). It was further established that hPRL-G129R-induced apoptosis is mediated through the inhibition of the antiapoptotic effects of hPRL via the downregulation of Bcl-2 gene expression (Beck *et al.*, 2002). In this study, evidence from breast cancer cells, as well as from transgenic mice,

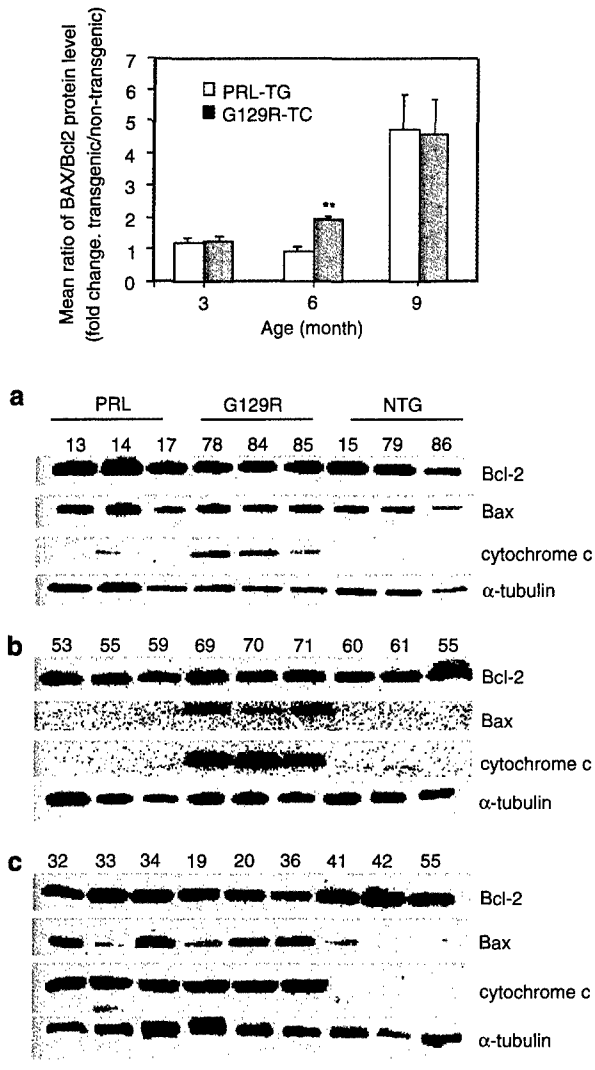

Figure 4 Western blot analyses of mammary gland homogenates from 3- (panel a), 6- (panel B) and 9-month (panel C) hPRL and hPRL-G129R transgenics and age-matched nontransgenic littermates. A measure of 50 μg of protein was loaded per well. Blots were hybridized first to an anti-Bcl-2 antibody, striped and were reprobed with antibodies specific to Bax, cytochrome *c*, and α-tubulin. Three nontransgenic age-matched littermates were chosen for each transgenic grouping. (Inset) Ratio of Bax and Bcl-2 protein calculated from densitometric scans of Bax and Bcl-2 protein levels in the Western blots of hPRL and hPRL-G129R transgenic animal tissue

is presented, which suggests that both Bax and Bcl-2 expression are regulated by hPRL-G129R.

The time course of Bax mRNA increase in response to hPRL-G129R treatment matched the response of *bcl-2* following PRL treatment in T-47D cells (Figure 1). It is widely accepted that the overall Bax/Bcl-2 status ultimately decides the apoptotic fate of the cell (Debatin *et al.*, 2002). The data presented in this study suggest that the balance is tipped in favor of apoptosis, following hPRL-G129R treatment in seven of these 11 cell lines (Figure 2c). In the examination of the entire panel of human breast cancer cell lines, it was found that the cell lines with highest response levels of *bcl-2* to hPRL treatment (MCF-7, T-47D and MDA-MB-134) also had the highest levels of *bax* in response to hPRL-G129R treatment (Figure 2). The cell lines that demonstrated decreased *bcl-2* responses to hPRL treatment (MDA-MB-436, MDA-MB-468, MDA-MB-231, BT-483) were also less responsive to treatment with hPRL-G129R. Not surprisingly, these cell lines also have lower PRLR levels (Peirce and Chen, 2002), suggesting that, in these cell lines, PRL plays a less significant role in the regulation of *bax* and *bcl-2* expression.

From our previous study, it is apparent that both the death receptor (Bcl-2-independent) pathway and the mitochondrial membrane permeabilization (MMP) pathway are represented in the microarray panel of four cell lines, and presumably in the larger panel of 11 breast cancer cell lines; the presence of these pathways is likely mirrored by the Bax/Bcl-2 and cytochrome *c* responses to hPRL and hPRL-G129R treatments. It is plausible that the proapoptotic PRL antagonist acts by slowing more aggressive growth by direct blockage of proliferative cascades, allowing the initiation of upregulation of possible apoptotic pathways; in particular, the c-jun N-terminal kinase (JNK) kinases have been suggested as possible candidates (Debatin *et al.*, 2002). In addition, the post-translational form of the hPRL protein may determine the signal transduction pathway(s) induced in each situation (MAPK-Ras/Raf *vs* Jak2/Stat), and hence the levels of Bax or Bcl-2. For example, PRL undergoes a number of post-translational modifications, most importantly phosphorylation. A molecular mimic of phosphorylated PRL has been found to be involved in differentiation, rather than proliferation, whereas the unphosphorylated form is primarily involved in proliferative processes (Kuo *et al.*, 2002).

From the *in vivo* studies, it is apparent that Bax, Bcl-2 and cytochrome *c* levels were under the dual influences of developmental and age-related changes, as well as the transgenes hPRL or hPRL-G129R. The real time RT–PCR data indicated a major increase in *bcl-2* levels in the hPRL group at 6 months and a major increase in *bax* levels in the hPRL-G129R group at 9 months relative to the nontransgenic littermates (Figure 3). However, the largest *bax*/*bcl-2* gene expression ratio is seen in the hPRL-G129R transgenics at 6 months (Figure 3b), and this is reflected in the release of cytochrome *c*; thus, gene expression is linked to an apoptotic outcome in this system. At the protein level, there was a major increase in Bax in the hPRL-G129R group at 6 months, accompanied by cytochrome *c* release (Figure 4b). There were major increases in Bax and cytochrome *c* release in the hPRL group of transgenics at 9 months (Figure 4c). At 6 months, overexpression of hPRL-G129R led to apoptotic processes, while overexpression of hPRL was linked to the upregulation of Bcl-2 mRNA. However, by 9 months, it is plausible that prolonged exposure to elevated levels of systemic hPRL led to a recapitulation of events seen in early involution. By accelerating events normally seen in PRL-induced proliferation (Brockman

et al., 2002), downregulation of PRLR levels may be triggered. This could lead to an accumulation of next-stage factors, namely those factors involved in apoptosis in lobule–alveolar tissues and induced by sequential exposure and subsequent withdrawal of lactogenic hormones such as PRL (Marti *et al.*, 1997). There was an apparent discrepancy in the concentrations of G129R needed to induce a significant response between our *in vitro* and *in vivo* models. We reasoned that, in the transgenic mice, the mammary gland is continually exposed to G129R and PRL, and that G129R is acting in an autocrine/paracrine manner; the low levels of PRL and G129R are sufficient to induce a significant response as compared to that of nontransgenic counterparts. However, the breast cancer cell lines used in this study were not only transformed and malignant, but have also been reported (T-47D cells) to produce PRL. Therefore, a much higher concentration of G129R was needed to induce a similar response.

In summary, the data presented here suggest that Bax is upregulated in response to hPRL-G129R stimulation both *in vitro* and *in vivo*; the expression of Bax is closely linked to cytochrome *c* release. However, the full extent of the Bax/Bcl-2 response may be modulated by other factors such as PRLR levels. The transgenic animal models that we have developed will allow us to evaluate pathways such as Jak2/Stat and Ras-MAPK in the context of such receptor levels, which are involved in the regulation of Bax and Bcl-2. Thus, apoptosis induced by hPRL-G129R in these breast cancer model systems is driven, at least in part, by the simultaneous downregulation of Bcl-2 and the upregulation of Bax at both the mRNA and protein levels, regulation that leads to the ultimate release of cytochrome *c*. In total, these data support the growing body of evidence of the potential importance of this PRL receptor antagonist for the treatment of breast cancer.

Materials and methods

Cell lines, growth conditions and treatments of cells for real-time RT–PCR

Five ER-positive (T47D, MDA-MDA-MB-134, BT-474, MDA-MB-483, MCF-7) and six ER-negative human breast cancer cell lines (BT-549, MDA-MDA-MB-231, MDA-MDA-MB-453, MDA-MB-468, MDA-MB-436 and MDA-MB-157) were obtained from the American Type Culture Collection (ATCC, Rockville, MD, USA) and maintained as previously described (Beck *et al.*, 2002).

Before treatment, the 11 breast cancer cell lines were transferred to their respective medium minus phenol red supplemented with 10% charcoal stripped serum (CSS) (Hyclone Laboratories, Logan, UT, USA) and grown for 1–2 days, reaching an approximate 75% level of confluency. Approximately $0.5-1 \times 10^7$ cells from each group were treated with 500 ng/ml of hPRL-G129R in medium containing 2% CSS. The untreated control cells were cultured in cell-specific medium supplemented with 2% CSS. All cells were treated for 48 h and harvested for total RNA extraction using the RNAqueous (Ambion, Austin, TX) RNA isolation kit, following the recommended protocol.

Transgenic mice and procedures

MT-regulated hPRL and hPRL-G129R cDNA were used to create hPRL and hPRL-G129R transgenic founder mice from the B6C3F1 strain (Jackson Labs, Bar Harbor, ME, USA) by microinjection into single-cell embryos. Transgenic mice were confirmed by PCR for the presence of hPRL and hPRL-G129R cDNAs (data not shown). The serum expression levels of hPRL and hPRL-G129R from the transgenic mice ranged from 5 to 10 ng/ml, as measured by a ^{125}I immunoradiometric serum assay, Coat-A-Count PRL IRMA (Diagnostic Products Corporation, LA, CA, USA). The human PRL IRMA assay is equally sensitive to hPRL and G129R (data not shown). To ensure the specificity of the measurement, nontransgenic mouse serum was used to generate a negative baseline. For the evaluation of Bax and Bcl-2 mRNA and protein expression, mice were grouped into three age categories: 3 months, 6–7 months and 9–12 months. Each group contained 4–6 hPRL or hPRL-G129R transgenic mice, and 2–4 white, nontransgenic littermates.

Isolation of total RNA from mouse mammary gland tissues

Fresh mammary gland tissue was flash-frozen on dry ice or in liquid N_2, and stored at −80°C until use. For RNA isolation, an approximate 50 mg portion of frozen tissue was added to 1 ml RNA lysis/binding buffer (Ambion, Austin, TX, USA). The tissue was homogenized using a Polytron PT 1200 B, and total RNA was extracted using the RNAqueous (Ambion) RNA isolation kit, following the recommended protocol. RNA was quantified by UV spectrophotometry.

One-step real-time RT–PCR

A one-step real-time RT–PCR technique was used to determine the relative expression levels of *bax* mRNA, using the ABI Perkin-Elmer Prism 7700 Sequence Detection System (Perkin-Elmer Biosystems, Foster City, CA, USA). The reaction mix included a 200 nm final concentration of both forward (derived from exon 3: 5′-CCGCCGTGGACACA-GAC-3′) and reverse (derived from exon 5: 5′-CAGAAAA-CATGTCAGCTGCCA-3′) *bax*-specific primers, and a 100 nm final concentration of the *bax*-specific FAM-labeled probe (5′-6FAM-CCCCCCGAGAGGTCTTTTTCCGAC-TAMRA-3′). For detection of *bcl-2* mRNA, the reaction mix included a predeveloped TaqMan assay mixture containing both forward and reverse *bcl-2*-specific primers, and a 100 mM final concentration of the *bcl-2*-specific probe labeled with FAM reporter fluorescent dye (Perkin-Elmer). A one-step reaction mixture provided in the TaqMan® Gold RT–PCR Kit (Perkin-Elmer) was used for all amplifications (5.5 mM $MgCl_2$, 50 mM KCl, 0.01 mM EDTA, 10 mM Tris-HCl pH 8.3, 300 μM deoxyATP, 300 μM deoxyCTP, 300 μM deoxyGTP, 600 μM deoxyUTP, 0.025 U/ml AmpliTaq Gold DNA polymerase, 0.25 U/ml MultiScribe Reverse Transcriptase, 0.4 U/ml RNase inhibitor). Cycle parameters for the one-step RT–PCR included a reverse-transcription step at 48°C for 30 min, followed by 40 cycles of 95°C denaturation and 60°C annealing/extension. In all, 400–1500 ng of total RNA was used per reaction. The housekeeping gene β-actin (Applied Biosystems P/N 401846) was used for internal normalization for RNA isolated from cell cultures; for expression from mammary gland tissue-derived RNA, 18s rRNA (Applied Biosystems PDAR-4310) was used for internal normalization. Each reaction was carried out in duplicate for each PCR run, and each run was repeated two to five times. Data are expressed as the means ± s.e.

Extraction of protein from mouse mammary gland tissue

Fresh mammary gland tissue was flash-frozen on dry ice or in liquid N_2, and stored at −80°C until use. For extraction of protein, an approximate 100–200 mg of frozen tissue was homogenized using a Polytron PT 1200 B in 4 ml of tissue homogenate buffer (50 mM Tris-HCl, pH 7.4; 1% NP-40; 0.25% sodium deoxycholate; 150 mM NaCl; 1 mM EDTA; 1 mM PMSF; 1 μg/ml aprotinin; 1 μg/ml leupeptin; 1 mM Na_3VO_4; 50 mM NaF and 1 μg/ml pepstatin). Homogenates were incubated overnight at 4°C on a vertical rotator, and the extracts were cleared by spinning in an Eppendorf cenrifuge at 20 800 RCF, twice at 4°C for 20 min. Supernatant was kept frozen at −20°C until use.

Preparation and analyses of cell lysates and protein homogenates for Bcl-2, Bax and cytochrome c *levels*

A measure of 50 μg of cell lysate or 15 μg of protein homogenate lysate (determined by spectrophotometric protein assays) was added to 3 × SDS-PAGE sample buffer. Samples were heated at 100°C and analysed on a 12% (Bax, Bcl-2) or 15% (cytochrome *c*) polyacrylamide gel (Bio-Rad; Hercules, CA, USA). Protein was transferred to a Hybond nitrocellulose membrane (Amersham, Arlington Heights, IL, USA) for 2.5 h at 12 W. A high molecular weight rainbow marker (Amersham) was used to confirm the protein size as well as the efficacy of transfer. Following transfer, the membranes were blocked overnight at 4°C in TBS containing 5% non-fat powdered milk and 0.05% Tween-20. Membranes were incubated with Bax antiserum (sc-493; Santa Cruz Biotechnology) at a 1 : 1000 dilution. A Bcl-2 monoclonal antibody (AM43; Oncogene Research Products, Boston, MA, USA) was used at a concentration of at 0.2 μg/ml for analysis of murine tissue; a Bcl-2 polyclonal antibody (sc-783; Santa Cruz Biotechnology, CA, USA) was used at a 1 : 1000 dilution for analysis of human breast cancer cells. A cytochrome *c* monoclonal antibody (sc-13560; Santa Cruz Biotechnology) was used at a 1 : 1000 dilution for analysis of murine tissue; a second cytochrome *c* monoclonal antibody (7H8.2C12; BD Transduction Laboratories, LA, CA, USA) was used at a 1 : 250 dilution in the analysis of cell lysates. The cytochrome *c* antibody was incubated overnight at 4°C with gentle agitation; all other antibodies were incubated for 1 h at 4°C with gentle agitation. Goat anti-mouse (Bcl-2, cytochrome *c*) or goat anti-rabbit (Bax) HRP-conjugated secondary antibodies (BioRad, Hercules, CA, USA) were diluted 1 : 2000, and the blots incubated for 2–4 h at room temperature. Bands were visualized using the ECL detection system (Amersham), as per the manufacturer's instructions. To confirm that equivalent amounts of total protein were added to each well, membranes were stripped by incubation in 100 mM β-mercaptoethanol/2% SDS/62.5 mM Tris-HCl pH 6.7 at 50°C for 30 min, and reprobed with an anti-α-actin monoclonal antibody (Sigma, St Louis, MO, USA) for analysis of the cell lysates, or an anti-β-tubulin monoclonal antibody (Sigma, St Louis, MO, USA) for analysis of the protein homogenates.

Quantitative analysis of Western blotting results

Western blotting images were saved as TIFF-type files and analysed using the BioRad densitometric analysis system Quantity One, following the instructions of the User Guide. After normalization to levels of α-tubulin, the densitometric values of the nontransgenic controls were designated as 100%, and other values were defined as percentages of these controls.

Statistical analyses

All values are given as means ± s.e. Statistical analyses were performed using the program StatsDirect version 1.9.8 (CamCode, Cambridge, England) with one-way ANOVA and a Tukey-multiple comparison test. *P*-values less than 0.01 were considered highly statistically significant and *P*-values between 0.01 and 0.05 were considered statistically significant.

Acknowledgements
We thank Dr Karl Franek for his careful review of this manuscript. This work was supported in part by the Endowment Fund of the Greenville Hospital System and grants from the US Army Medical Research Command (DAMD17-99-1-9129 and DAMD17-01-1-0207) and NIH/NCI (CA87093).

References

Adams JM and Cory S. (1998). *Science*, **281,** 1322–1326.
Beck MT, Peirce SK and Chen WY. (2002). *Oncogene*, **21,** 5047–5055.
Ben-Jonathan N, Liby K, McFarland M and Zinger M. (2002). *Trends Endocrinol. Metab.*, **13,** 245–250.
Bhatavdekar JM, Patel DD, Shah NG, Vora HH, Suthar TP, Ghosh N, Chikhikar PR and Trivedi TI. (2000). *Eur. J. Surg. Oncol.*, **26,** 540–547.
Binart N, Ormandy CJ and Kelly PA. (2000). *Adv. Exp. Med. Biol.*, **480,** 85–92.
Binder C, Marx D, Binder L, Schour A and Hiddemann W. (1996). *Ann. Oncol.*, **7,** 129–133.
Blackwell RE and Hammond KR. (1999). *Hormonal Control of Normal Breast Morphology and Function*, Manni A (ed). Humana Press: New Jersey, pp. 3–20.
Brockman JL, Schroeder MD and Schuler LA. (2002). *Mol. Endocrinol.*, **16,** 774–784.
Chen NY, Holle L, Li W, Peirce SK, Beck MT and Chen WY. (2002). *Int. J. Oncol.*, **20,** 813–818.
Chen WY, Ramamoorthy P, Chen NY, Sticca RP and Wagner TE. (1999). *Clin. Cancer Res.*, **5,** 3583–3593.
Clevenger CV, Chang WP, Ngo W, Pashe TLM, Montone KT and Tomaszewski JE. (1995). *Am. J. Pathol.*, **146,** 695–705.
Clevenger CV, Furth PA, Hankinson SE and Schuler LA. (2003). *Endocrine Rev.*, **24,** 1–27.
Corbacho AM, Martinez De La Escalera G and Clapp C. (2002). *J. Endocrinol.*, **175,** 219–238.
Cory S and Adams JM. (2002). *Nat. Rev.*, **2,** 647–656.
Debatin KM, Poncet D and Kroemer G. (2002). *Oncogene*, **21,** 8786–8803.
Ginsburg E and Vonderhaar BK. (1995). *Cancer Res.*, **55,** 2591–2595.
Green DR and Beere HM. (1999). *Apoptosis and Cancer Chemotherapy: Mechanisms of Apoptosis*, Hickman JA and Dive C (ed). Humana Press: New Jersey, pp. 157–174.
Korsmeyer SJ. (1999). *Cancer Res.*, **59,** 1693–1700.
Krajewski S, Krawjewska M, Turner BC, Pratt C, Howard B, Zapata JM, Frenkel V, Robertson S, Ionov Y, Yamamoto

H, Perucho M, Takayama S and Reed JC. (1999). *Endocr. Relat. Cancer*, **6,** 29–40.

Krumenacker JS, Buckley DJ, Leff MA, McCormack JT, de Jong G, Gout PW, Reed JC, Miyashita T, Magnuson NS and Buckley AR. (1998). *Endocrine*, **2,** 163–170.

Kumar R, Vadlamundi RK and Adam L. (2000). *Endocr. Relat. Cancer*, **7,** 257–269.

Kuo CB, Wu W, Xu X, Yang L, Chen C, Coss D, Birdsall B, Nasseri D and Walker AM. (2002). *Cell Tissue Res.*, **309,** 429–437.

Marti A, Feng Z, Altermatt HJ and Jaggi R. (1997). *Eur. J. Cell. Biol.*, **73,** 158–165.

Nagasawa H, Miur K, Niki K and Namiki H. (1985). *Exp. Clin. Endocrinol.*, **86,** 357–360.

Peirce SK and Chen WY. (2001). *J. Endocrinol.*, **17,** R1–R4.

Schorr K, Li M, Bar-Peled U, Lewis A, Heredia A, Lewis B, Knudson CM, Korsmeyer SJ, Jager R, Weiher H and Furth PA. (1999). *Cancer Res.*, **59,** 2541–2545.

Vonderhaar BK. (1999). *Endocr. Relat. Cancer*, **6,** 389–404.

Vonderhaar BK. (1998). *Pharmacol. Ther.*, **79,** 169–178.

Wennbo H, Kindblom J, Isaksson OG and Tornell J. (1997). *Endocrinology*, **138,** 4410–4415.

Yin XM, Oltvai ZN and Korsmeyer SJ. (1994). *Nature*, **369,** 321–323.

Zhang H, Xu S, Krajewski M, Krajewski Z, Xie S, Fuess S, Kitada S, Pawlowski A, Godzik A and Reed JC. (2000). *Proc. Natl. Acad. Sci. USA*, **97,** 2597–2602.

[CANCER RESEARCH 63, 3598–3604, July 1, 2003]

Prolactin Antagonist-endostatin Fusion Protein as a Targeted Dual-Functional Therapeutic Agent for Breast Cancer[1]

Michael T. Beck, Nian Y. Chen, Karl J. Franek, and Wen Y. Chen[2]

Department of Biological Sciences, Clemson University, Clemson, South Carolina 29634 [M. T. B., K. J. F., W. Y. C.]; Oncology Research Institute, Greenville Hospital System, Greenville, South Carolina 29605 [M. T. B., K. J. F., W. Y. C.]; and Department of Biology, Converse College, Spartanburg, South Carolina 29302 [N. Y. C.]

ABSTRACT

In previous studies (Chen, W. Y. *et al.*, Clin. Cancer Res., *5:* 3583–3593, 1999; Chen, N Y. *et al.*, Int. J. Oncol., *20:* 813–818, 2002), we have demonstrated the ability of the human prolactin (hPRL) antagonist, G129R, to inhibit human breast cancer cell proliferation *in vitro* and to slow the growth rate of tumors in mice. We further revealed that the possible mechanisms of G129R antitumor effects act through the induction of apoptosis via the regulation of *bcl-2* gene expression. It has been established that to sustain tumor growth, it is necessary for the development of a network of blood vessels to bring in nutrients, a process called angiogenesis. The disruption of angiogenesis has been proven to be an effective strategy to cause regression of certain tumors. One of the best-studied angiogenesis inhibitors is endostatin, which acts through the inhibition of endothelial cells. In this study, we combine the anti-breast tumor effects of G129R and the antiangiogenic effects of endostatin by creating a novel fusion protein (G129R-endostatin) specifically for breast cancer therapy. The data presented here demonstrated that this novel fusion protein was able to bind to the PRL receptor (PRLR) on T-47D human breast cancer cells and inhibit the signal transduction induced by PRL. At the same time, G129R-endostatin inhibited human umbilical vein endothelial cell (HUVEC) proliferation and disrupted the formation of endothelial tube structures with potency similar to that of endostatin. More importantly, the therapeutic efficacy of G129R-endostatin was confirmed using a mouse breast cancer cell line 4T1 *in vivo*. G129R-endostatin has a significantly prolonged serum half-life as compared with that of G129R or endostatin alone, and exhibited greater tumor inhibitory effects than G129R and endostatin individually or in combination. Taken together, these data demonstrate the dual therapeutic effects of G129R-endostatin, and suggests that this fusion protein has great promise as a novel anti-breast cancer agent.

INTRODUCTION

Human breast cancer affects ~1.1 million women per year, and ~35% of these new cases will eventually result in death. Tumor metastasis still remains the main cause of breast cancer deaths (1). Although with chemotherapy and radiation therapy, the prognosis has improved in some cases, these approaches may result in severe side effects. Recently, PRL[3] has become one of the focal points in the investigation into the mechanism and onset of human breast cancer (2, 3). hPRL has been linked to breast cancer by several lines of evidence: (*a*) an autocrine/paracrine loop for hPRL has been demonstrated with the finding of biologically active PRL in breast cancer cells (2, 4–7); (*b*) PRLR expression levels are up-regulated in breast cancer cells and neoplastic mammary tissues (8); (*c*) there is a high breast cancer rate in transgenic mice overexpressing lactogenic hormones (9); and (*d*) inhibition of PRL activity with an antagonist inhibits the proliferation of breast cancer cells both *in vitro* (10) and in mouse studies (11). In view of these studies, it is evident that PRL plays an important etiological role in breast cancer, and that the development of a PRL receptor antagonist may have potential as a therapeutic agent in treating this disease.

In previous studies, it was demonstrated that a single amino acid substitution mutation in hPRL resulted in a PRLR antagonist, G129R (5, 10). We have further determined that G129R inhibits human breast cancer cells through the induction of apoptosis (10). One of the key mechanisms that controls signal transduction of breast cancer cells is the stimulation of the JAK/STAT/mitogen-activated-protein-kinase (MAPK) pathways by PRL. Our previous work has shown that G129R inhibits human breast cancer proliferation, at least in part, through the inhibition of STATs phosphorylation (12). In addition, hPRL up-regulates the proapoptotic gene *bcl-2*, and G129R competitively down-regulates the *bcl-2* gene expression in human breast cancer cells (13). Furthermore, anti-breast tumor effects of G129R were confirmed by using human breast cancer xenografts in nude mice (11). These studies provide strong evidence for the ability of G129R to inhibit human breast cancer and the potential to become a therapeutic agent for the treatment of human breast cancer.

A key factor in the maintenance of the uncontrollable growth of cancer cells is the formation of new blood vessels in the tumor mass to provide nutrients, namely tumor angiogenesis (14–17). Angiogenesis is also required for tumor metastasis to occur and, thus, the inhibition of tumor angiogenesis holds great promise as a therapeutic approach in stopping primary tumor growth and metastasis (18). In recent years, there have been several inhibitors of angiogenesis identified including thrombospondin (TSP-1), angiostatin, protamine, and endostatin (19, 20). Endostatin is a M_r 20,000 COOH-terminal fragment of collagen XVIII and was first characterized in murine EOMA cells by O'Reilly *et al.* (21) and was later characterized in humans (22). Endostatin is a specific inhibitor of endothelial cell proliferation and is a potent inhibitor of angiogenesis (23–25). Although the mechanism of endostatin activity is not fully understood, the crystal structure of endostatin reveals a heparin sulfate-binding site (26), suggesting that endostatin can inhibit such heparin-binding angiogenic factors as bFGF-2. Murine tumors that are dependent on angiogenesis for growth were successfully regressed to microscopic lesions after systemic therapy with murine endostatin (21). Such inhibition may lead to tumor dormancy as a result of an increased level of apoptosis in endothelial cells (27). Recently, Phase I clinical trials of endostatin have been completed, and it is currently in Phase II studies. In this study, we combined the tumor targeting and inhibitory activities of G129R with the antiangiogenic abilities of endostatin by creating a novel fusion protein (G129R-endostatin), and tested its potential dual therapeutic effects both in cell culture as well as in mouse tumor models.

MATERIALS AND METHODS

Cell Lines and Growth Conditions. The human breast cancer cell line T-47D, mouse breast cancer cell line 4T1, and HUVECs were purchased from the American Type Culture Collection (Manassas, VA). T-47D cells were maintained in RPMI 1640 (Life Technologies, Inc., Gaithersburg, MD) supplemented with 10% FBS (Hyclone Laboratories, Logan, UT) and 100 μg/ml

Received 10/16/02; accepted 4/28/03.

The costs of publication of this article were defrayed in part by the payment of page charges. This article must therefore be hereby marked *advertisement* in accordance with 18 U.S.C. Section 1734 solely to indicate this fact.

[1] Supported in part by the Endowment Fund of the Greenville Hospital System, United States Army Medical Research Command Grant DAMD17-99-1-9129), and NIH/National Cancer Institute Grant 1R21CA87093.

[2] To whom requests for reprints should be addressed, at Oncology Research Institute, Greenville Hospital System, Greenville, South Carolina 29605. Phone: (864) 455-1457; Fax: (864) 455-1567; E-mail: wchen@ghs.org.

[3] The abbreviations used are: PRL, prolactin; hPRL, human PRL; PRLR, hPRL receptor; bFGF, basic fibroblast growth factor; HUVEC, human umbilical vein endothelial cell; FBS, fetal bovine serum; IRMA, immunoradiometric assay; TBS, Tris-buffered saline; ECM, extracellular matrix.

gentamicin (Hyclone). 4T1 cells were maintained in RPMI 1640 supplemented with 10% FBS, 1% sodium pyruvate (Life Technologies, Inc.), 100 μg/ml gentamicin, 4.5 g/liter glucose (Sigma, St. Louis, MO), and 1 mM HEPES (Life Technologies, Inc.). HUVECs were maintained in Medium-199 supplemented with 10% FBS, 100 μg/ml gentamicin, and an EGM-2 Singelquot (Cambrex, East Rutherford, NJ). Cells were grown at 37°C in a humid atmosphere in the presence of 5% CO_2.

Cloning and Expression of G129R-Endostatin Fusion Protein. A two-step cloning procedure was used to generate a recombinant cDNA encoding G129R fused to human endostatin. Primers corresponding to G129R (5′ primer; restriction site for *Nde*I underlined, 5′-CAT ATG TTG CCC ATC TGT CCC GGC-3′, and 3′ primer, restriction site for *Bam*HI underlined, 5′-GGA TCC GCA GTT GTT GTT GTG GAT-3′) were used to amplify the G129R fragment from a previous clone (10). Primers corresponding to human endostatin (5′ primer; restriction site for *Bam*HI underlined, 5′-GGA TCC CAC AGC CAC CGC GAC TTC CAG-3′, and 3′ primer, restriction site *Xho*I with stop codon underlined, 5′-CTC GAG CTA CTT GGA GGC AGT CAT GAA GC-3′) were used to amplify the gene from a Human Universal QUICK-Clone cDNA library (Clontech, Palo Alto, CA). Another 5′ primer, *Nde*I, 5′-CAT ATG CAC AGC CAC CGC GAC TTC CAG, was used with the *Xho*I 3′ primer for expression of human endostatin alone. All of the cDNA fragments were ligated separately into the TA cloning vector pCR2.1 (Invitrogen, Inc., Carlsbad, CA), were restriction mapped, and were sequenced. The cDNA fragments were restriction digested at the cloned restriction sites, were purified, and were ligated into the protein expression vector pET22b(+) (Novagen, Madison, WI) for the expression of G129R-endostatin and endostatin proteins. The design of the fusion protein is such that the NH_2-terminal portion of endostatin is ligated to the COOH-terminal portion of G129R.

Production and Purification of Endostatin, G129R, and G129R-Endostatin Fusion Protein. G129R was purified as described previously (10). Endostatin and G129R-endostatin were purified according to Huang *et al.* (28). Briefly, BL21 (Novagen) chemically competent cells were transformed with pET22b(+) vector encoding for endostatin, G129R, and G129R-endostatin cDNA. Bacteria were allowed to grow overnight in Luria-Bertani broth (ampicillin, 50 μg/ml) at 37°C. The next day the bacteria were induced with isopropyl-beta-D-thiogalactopyranoside (IPTG) for 5 h to induce protein expression. Bacteria were collected and were resuspended in 100 ml of buffer A [0.1 M Tris-HCl (pH 8.0) and 5 mM EDTA], followed by incubation at room temperature for 15 min, with the addition of lysozyme at a final concentration of 50 μg/ml. The suspension was then sonicated using a 550 Sonic Dismembrator (Fisher Scientific, Pittsburgh, PA) in the presence of 0.1% sodium deoxycholate, followed by centrifugation at 8000 × *g* for 10 min. The pellet was resuspended in 100 ml of buffer A containing 0.1% sodium deoxycholate. The centrifugation/resuspension procedure was repeated twice. The pellet was dissolved in 30 ml of buffer B [0.05 M Tris (pH 8.0), 1% SDS, and 1 mM DTT] and was centrifuged at 8000 × *g* for 10 min at 4°C. The clear supernatant obtained was then transferred to dialysis tubing with a M_r cutoff of 10,000 and was dialyzed twice in 1500 ml of buffer C [0.05 M Tris-HCl (pH 8.0) and 0.1 mM DTT] at 4°C for 4 h. The recombinant protein was then further dialyzed twice in 1500 ml of buffer D [0.05 M Tris-HCl (pH 8.0)] and twice in 1000 ml of buffer E [0.05 M Tris-HCl (pH 8.0), 0.01 mM oxidized glutathione, and 1 mM reduced glutathione] at 4°C for 4 h/dialysis cycle, respectively. A final dialysis in 0.05 M Tris-HCl (pH 8.0) was performed overnight. Both endostatin and G129R-endostatin were soluble in the dialysis buffer. The G129R protein was purified on a fast-performance liquid chromatography system (FPLC; Amersham Pharmacia, Newark, NJ) after refolding as described previously (12). The endostatin and G129R-endostatin fusion protein preparations contain ~400 EU/mg protein and G129R preparation contains <5 EU/mg protein as tested by the Gel-Clot method (Cape Cod, Inc). The concentration of G129R, endostatin, and G129R-endostatin was determined by the Bio-Rad protein assay method (Bio-Rad, Hercules, CA) and G129R and G129R-endostatin were further verified using a hPRL IRMA kit (DPC, Inc., Los Angeles, CA). The purity of the proteins was determined on a SDS-PAGE gel stained with Coomassie Blue (Fisher Scientific).

Immunoblot Analysis. G129R, endostatin, and G129R-endostatin were separated on a 4–15% SDS-PAGE gel. The proteins were transferred to enhanced chemiluminescence Hybond nitrocellulose (Amersham Pharmacia) at 12 W for 2 h. The nitrocellulose blot was blocked with TBS containing 0.05% Tween 20 and 5% milk (blocking buffer) for 1 h at room temperature. Blots were incubated overnight at 4°C in blocking buffer containing the appropriate antibody [rabbit antihuman endostatin, 1:200 (Oncogene Research Products, San Diego, CA); rabbit anti-hPRL antiserum, 1:1000 (Dr. A. Parlow, National Hormone and Pituitary Program, NIH, Bethesda, MD)]. The blots were washed three times, 5 min each, with TBS containing 0.05% Tween, and were incubated with the secondary antibody goat-antirabbit horseradish peroxidase (1:5000; Bio-Rad) for 2 h at room temperature with gentle agitation. Blots were washed three times, 5 min each, with TBS containing 0.05% Tween and were developed for 1 min using the ECL Western detection reagents (Amersham Pharmacia). Immunoblots were visualized using Kodak MR film (Fisher).

Radioreceptor Binding Assay. T-47D human breast cancer cells expressing the PRL receptor were grown to confluency (~10^5 cells/well) in six-well tissue culture plates. Cells were starved in serum-free RPMI 1640 for 1 h, and then were incubated for 2 h at room temperature in serum-free RPMI medium containing ^{125}I-labeled hPRL (specific activity, 40 μCI/μg; NEN Perkin-Elmer, Boston, MA) with or without various concentrations of PRL, G129R, endostatin, and G129R-endostatin. Cells were washed three times with serum-free RPMI medium and were lysed in 0.5 ml of 0.1 N NaOH/1% SDS. The bound radioactivity was determined by scintillation counting, and the percentage of specific displacement was calculated and compared among these samples.

Immunofluorescence Staining. T-47D cells and HUVECs were maintained as described previously. Cells were passed onto Lab-Tek Chamber Slide System (Fisher) and were grown to ~70% confluency. HUVECs were cultured in low-serum medium (2% FBS), and T-47D cells were serum depleted for 30 min. Cells were treated with 10 μg/ml (435 nM) of G129R, 10 μg/ml (500 nM) of endostatin, or 20 μg/ml (476 nM) of G129R-endostatin for 30 min at 37°C. Cells were treated in their respective serum-free media, and all of the staining was performed in triplicate and repeated at least twice. After treatment, cells were washed with PBS [120 mmol NaCl; 2.7 mmol KCl; and 10 mmol phosphate buffer salts (pH 7.4)], fixed with 4% *para*-formaldehyde (BD Biosciences, Bedford, MA) for 25 min at 4°C, and permeabilized with 0.2% Triton X-100 in 1× PBS. Cells were incubated in blocking buffer for 30 min with 2% BSA (Fisher). Cells were incubated with the primary antibodies rabbit antihuman endostatin (Ab-2), 1:200, and mouse anti-hPRL antiserum, 1:1000, at room temperature for 2 h. After incubation, cells were washed three times with 1% BSA/PBS and subjected to secondary antibody (1:500) incubation for 2 h at room temperature using Alexa Fluor 594 goat antimouse IgG (red fluorescence) and Alexa Fluor 488 goat antirabbit IgG (green fluorescence; Molecular Probes, Inc., Eugene, OR), respectively. Cells were rinsed twice with 1% BSA/PBS and incubated with Anti-Fade equilibrium buffer (10 μl/well; Molecular Probes) for 10 min at room temperature. The chambers were then removed and cover slides were mounted for observation. All of the wells were examined under an Zeiss LSM 510 confocal microscope using 488-nm and 594-nm wavelengths. Digital photographs were taken at ×450.

STAT-5 Phosphorylation Assay. T-47D cells were grown to 80% confluency in six-well plates in RPMI 1640 containing 10% charcoal-stripped FBS. On the day of the experiment, cells were depleted for 30 min in RPMI 1640 containing 0.5% charcoal-stripped FBS. Cells were then treated for 20 min with the appropriate amount of PRL, G129R, endostatin, G129R-endostatin, or a combination treatment as indicated in Fig. 4. Cells were washed with ice-cold PBS and were lysed with 200 μl of lysis buffer [50 mM Tris-HCl (pH 7.4), 1% NP40, 0.25% sodium deoxycholate, 150 mM NaCl, 1 mM EGTA, 1 mM phenylmethylsulfonyl fluoride, 1 μg/ml aprotinin, 1 μg/ml leupeptin, and 1 mM Na_3VO_4] and were incubated on an orbital shaker for 10 min at room temperature. The lysate was transferred to a sterile 1.5-ml centrifuge tube, gently passed through a 21-gauge needle six times, and then incubated on ice for 20 min. The lysate was centrifuged at 12,000 × *g* for 20 min at 4°C. The supernatant was removed, and 30 μl of the lysate (65–70 μg) was used for Western blotting analysis as described earlier, with the exception that anti-STAT5A + anti-STAT5B [1:4000; Upstate Biotechnology Inc. (UBI), Lake Placid, NY] or anti-phospho-STAT5 (1:5000; UBI) were substituted as the primary antibodies.

Cell Proliferation Assay. HUVEC's and T-47D cells were grown in their respective media free of phenol-red. Fully confluent HUVEC and T-47D cell cultures were trypsinized, and cells were resuspended in medium containing 5% FBS. Cells were then seeded into 96-well culture plates at a density of 5,000 HUVECs/well [in the presence of 2.5 ng/ml bFGF (Sigma) and 1 μg/ml heparin (Sigma)] and 15,000 T-47D cells/well. After an incubation of 24 h, various concentrations of G129R, endostatin, or G129R-endostatin were added to the appropriate well. Cells were further incubated for 72 h at 37°C in a

humidified 5% CO_2 incubator. The viability of the cells was determined using the MTS-PMS (CellTiter 96 Aqueous kit; Promega Corp., Madison, WI) colorimetric assay (following the manufacturer's instructions), and absorbance at 490 nm was determined using a microplate reader (Bio-Rad). Cell survival was calculated as a percentage of the control values. All of the experiments were carried out in triplicate.

Endothelial Tube Formation Assay. Matrigel (BD Biosciences) was added (320 μl) to each well of a 24-well plate and allowed to polymerize at room temperature for 20 min. A suspension of 30,000 HUVECs/well in 300 μl of Medium 199 containing EGM-2 without antibiotics was transferred into each well. The cells were then treated with a low (100 ng/ml) and high (1000 ng/ml) concentration of G129R (4.3 nM, 43 nM), endostatin (5 nM, 50 nM), or G129R-endostatin (2.4 nM, 24 nM). All assays were performed in triplicate and were repeated at least twice. Cells were incubated for 24–48 h at 37°C in a humidified 5% CO_2 incubator were and observed using a CK2 Olympus microscope (3.3 ocular, ×10 objective).

Pharmacokinetic Study. Female BALB/c mice (Jackson Lab, Bar Harbor, ME) were used to determine the serum-effective dose of G129R-endostatin after a single i.p injection. Two hundred μg of G129R (8.7 nmol), 200 μg of G129R-endostatin (4.8 nmol), or 200 μg (10 nmol) of endostatin was injected (i.p.) into BALB/c mice (n = 4). Blood samples were obtained from each mouse at time intervals of 2, 4, 8, and 24 h by tail vein bleeding. Samples were placed on ice and immediately centrifuged for 5 min at 4°C. The serum was collected and frozen at −20°C until further use. The serum concentration of both G129R and G129R-endostatin was determined using the hPRL IRMA kit (DPC, Inc.). Endostatin serum concentration was determined using the Accucyte ELISA method (Oncogene). Area under the curve (*AUC*) was calculated by linear trapezoidal method from 2 to 24 h.

Antitumor Effects *in Vivo*. The *in vivo* antitumor efficacy of G129R-endostatin was examined using a 4T1 mouse mammary xenograft in an athymic nude mouse model. Female athymic nude (*nu/nu*) mice (Jackson Lab) 6–8 weeks of age were randomly placed into groups of 5 mice/cage, two cages/treatment for a total of 10 mice/group. 4T1 breast cancer cells (5×10^4) were injected s.c. into the mammary fat pad of each mouse, and tumors were allowed to develop for 5 days. Once tumors were established, mice were subjected to daily i.p. injections of different agents as designed. Treatment groups were given G129R [2.5 mg (110 nmol)/kg/day], endostatin [2.5 mg (125 nmol)/kg/day], G129R-endostatin [5 mg (130 nmol)/kg/day], and a combination of G129R (2.5 mg/kg/day) and endostatin (2.5 mg/kg/day) in a volume of 100 μl. Control groups were given 100-μl injections of sterile PBS. Measurements of tumors were recorded every 5 days until it was decided that tumors were debilitating to the mice. The long axis (*L*) and the short axis (*S*) were measured, and the tumor volume (*V*) was calculated using the following equation:

$$V = \frac{S^2 \times L}{2}$$

Once final measurements were taken, the mice were sacrificed by cervical dislocation, and tumors were dissected, weighed, and flash-frozen and were stored in liquid nitrogen until analysis.

Statistical Analysis. The results from the MTS assay and the animal studies were presented as means ± SE (*error bars*). Statistical analysis was performed using the program StatsDirect, version 1.9.8 (CamCode, Cambridge, England) with one-way ANOVA and a Tukey-Multiple Comparison test.

RESULTS

Expression of G129R-Endostatin Fusion Protein. The recombinant fusion protein along with G129R and endostatin were purified from the inclusion bodies of *Escherichia coli* cells. As shown in Fig. 1*A*, all of the recombinant proteins migrate as a single band during SDS gel electrophoresis under reduced conditions in predicted sizes (G129R-endostatin, M_r 42,000; G129R, M_r 23,000; endostatin, M_r 20,000). Western blot analysis was used to further confirm the presence of both G129R and endostatin in the G129R-endostatin fusion protein (Fig. 1*B*).

G129R-Endostatin Binds to Both Human Breast Cancer and Endothelial Cells. The ability of G129R-endostatin to directly bind to the PRLR on the human breast cancer cell line T-47D was demonstrated using a radioreceptor binding assay (Fig. 2). It was determined that PRL, G129R, and G129R-endostatin all competitively displaced the ^{125}I-labeled hPRL from the PRLR on T-47D cells with similar affinity, whereas endostatin did not, suggesting that G129R-endostatin retained its ability to recognize PRLR.

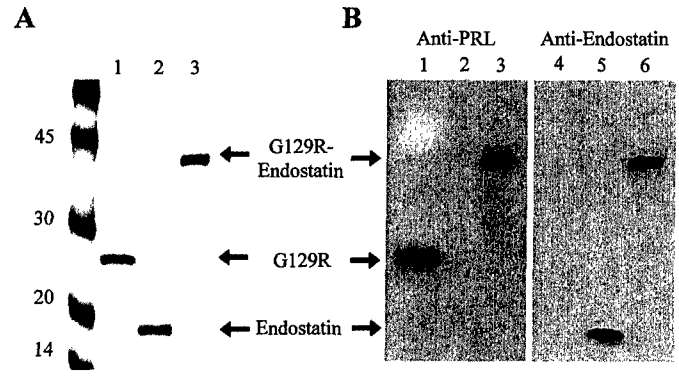

Fig. 1. Production and expression of G129R-endostatin. G129R and endostatin were cloned into the pET22b(+) expression vector. *A*, SDS-PAGE analysis of G129R-endostatin stained with Coomassie Blue. *At left*, molecular weight markers (kDa) in thousands. G129R migrates at M_r 23,000 (*Lane 1*) and endostatin at M_r ~20,000 (*Lane 2*). G129R-endostatin migrated at M_r ~43,000 (*Lane 3*). *B*, Western blot analysis of G129R-endostatin. *Lanes 1* and *4*, G129R; *Lanes 2* and *5*, endostatin; *Lanes 3* and *6*, G129R-endostatin. The left blot, *Lanes 1–3*, was incubated with a polyclonal rabbit anti-hPRL antibody and the right blot, *Lanes 4–6*, was incubated with a polyclonal rabbit antiendostatin antibody. A goat antirabbit IgG horseradish peroxidase conjugate was used as secondary antibody and was detected with ECL.

An immunofluorescence assay was used to determine whether G129R-endostatin can bind to both breast cancer and endothelial cells (Fig. 3). HUVEC and T-47D cells were treated with G129R, endostatin, or G129R-endostatin and were stained with protein-specific primary antibodies. Fluorescent secondary antibodies were used to distinguish G129R (Alexa Flour 594, Red) and endostatin (Alexa Flour 488, Green). Fig. 3, *A* and *B* represent the untreated HUVECs and T-47D cells as controls. As shown in Fig. 3, *C* and *D*, G129R-endostatin bound to HUVEC and T-47D cells, respectively. This is demonstrated by the fluorescence of both the endostatin antibody (*green*) and the PRL antibody (*red*) in the same field of view. Endostatin bound to HUVECs (Fig. 3*E*) and bound to what appears to be the ECM of T-47D cells with a scattered staining pattern (Fig. 3*F*). In contrast, G129R bound only to T-47D cells (Fig. 3*H*), but it did not bind to HUVECs (Fig. 3*G*). The distinct pattern of staining of G129R and endostatin is notable. G129R and G129R-endostatin treatments revealed a clear cellular staining pattern in T-47D cells (Fig. 3, *D* and *H*), whereas endostatin-treated cells demonstrated a scattered staining pattern in both HUVECs and T-47D cells (Fig. 3, *C*, *E*, and *F*). Because G129R did not bind to HUVECs caused by the lack of PRLR on these cells (Fig. 3*G*), the staining of HUVECs by G129R-endostatin (Fig. 3*C*) was most likely caused by the binding of the endostatin portion of the fusion protein.

G129R-Endostatin Inhibits STAT5 Phosphorylation in T-47D Human Breast Cancer Cells. STAT5 phosphorylation is one indicator of PRL-mediated signal transduction in mammary cells, and we have used this feature as a measure of the antagonistic effects of G129R and its variants (12). The status of STAT5 phosphorylation was examined after treatment of T-47D cells with PRL, G129R, endostatin, and G129R-endostatin. As shown in Fig. 4*A*, PRL (100 ng/ml, 4.3 nM) induced phosphorylation of STAT5 (pSTAT5), whereas G129R, endostatin, and G129R-endostatin, as expected, lacked the ability to induce STAT5 phosphorylation. A dose-dependent competitive inhibition of PRL-induced STAT5 phosphorylation was observed for G129R and G129R-endostatin (Fig. 4*B*). G129R and G129R-endostatin exhibited similar potency in the inhibition of

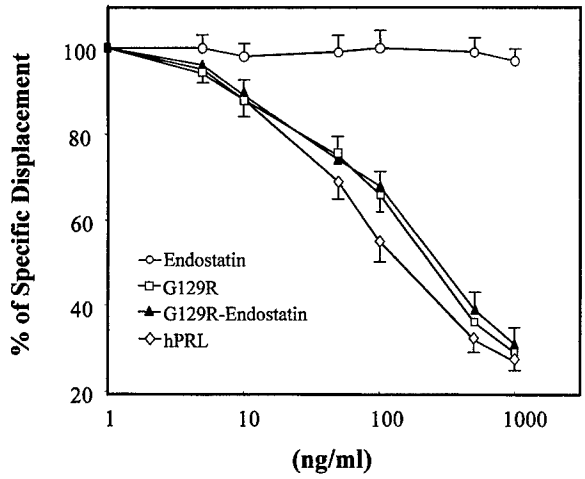

Fig. 2. Binding ability of G129R-endostatin to the PRL receptor on human breast cancer cells. The concentrations of the treatments are given on a log scale. The data are represented as the percentage of the displacement of ^{125}I-labeled hPRL (specific activity, 40 μCl/μg) compared with the total binding of each protein to human breast cancer cell line T-47D. The data represents the mean ± SD of three experiments.

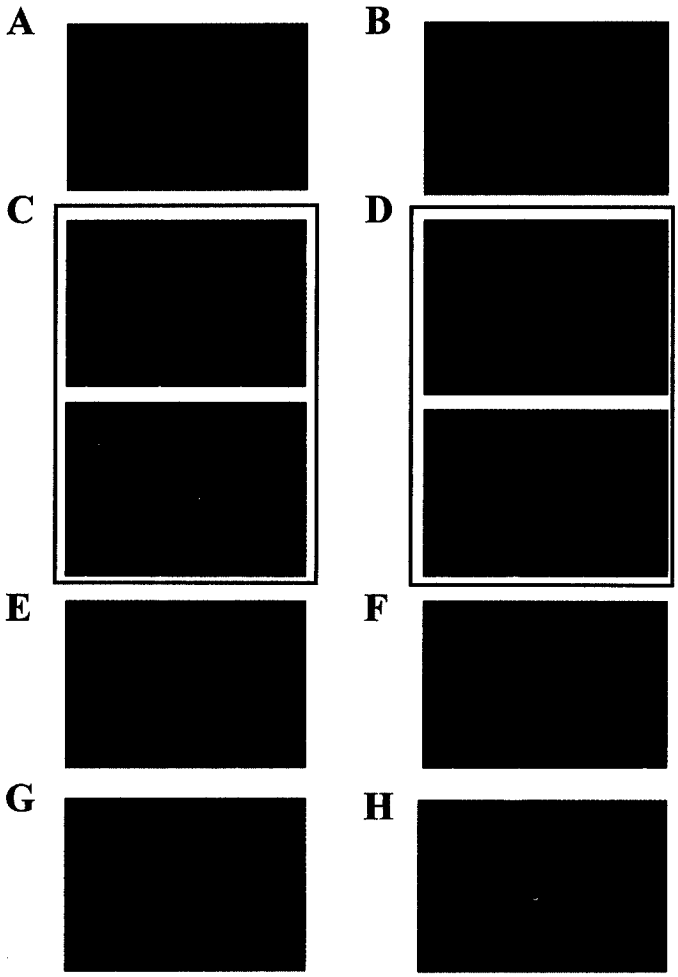

Fig. 3. Immunofluorescence staining of HUVECs and T-47D cells. *C* (HUVECs) and *D* (T-47D) represent cells treated with G129R-endostatin and stained with anti-hPRL and anti-human endostatin. *C* and *D* are boxed to represent the same field of view. Both *E* (HUVEC) and *F* (T-47D) represent cells treated with endostatin and G129R and stained with antihuman endostatin. Both HUVECs (*G*) and T-47D (*H*) cells were treated with endostatin and G129R and stained with anti-hPRL. Negative controls of HUVECs and T-47D cells were presented as *A* and *B*, respectively. The secondary antibodies used were Alexa Fluor 594 goat antimouse IgG (*red fluorescence*, PRL) and Alexa Fluor 488 goat antirabbit IgG (*green fluorescence*, endostatin), respectively, for each primary antibody. Digital photographs were taken at ×450.

STAT5 phosphorylation. This demonstrates that the G129R portion of G129R-endostatin retained its antagonistic effects toward PRLR.

G129R-Endostatin Inhibits the Proliferation of Human Endothelial and Human Breast Cancer Cells. Cell proliferation assays were carried out to examine the dual effects of G129R-endostatin in inhibiting the proliferation of both HUVECs and T-47D cells. G129R-endostatin was revealed to be as effective as endostatin in inhibiting the proliferation of HUVECs in a dose-dependent manner (Fig. 5*A*). The EC_{50} of G129R-endostatin (12 nM) was approximately one-half that of endostatin (25 nM; ~500 ng/ml; Fig. 5*A*). G129R had no effect on HUVEC proliferation, suggesting that the inhibitory effect of G129R-endostatin was caused by the endostatin domain of the fusion protein. Conversely, G129R-endostatin (EC_{50}, 18 nM) exhibited antiproliferative effects on T-47D human breast cancer cells similar to that of G129R (EC_{50}, 32 nM; ~750 ng/ml; Fig. 5*B*). As expected, endostatin had no effect on the proliferation of T-47D cells. Overall, G129R-endostatin was effective in inhibiting T-47D and HUVEC growth at molar concentrations much lower than those of G129R or endostatin, respectively.

G129R-Endostatin Fusion Protein Disrupts the Formation of Endothelial Tubes. An endothelial tube formation assay was used to further confirm the antiangiogenic activity of G129R-endostatin. In this experiment, the use of Matrigel permits the growth and differentiation of endothelial cells into tubal structures that are reminiscent of blood vessels. Prominent tubal structures were observed in the control cells (Fig. 6). At low concentrations (100 ng/ml; Fig. 6, *left column*) both endostatin and G129R-endostatin began to disrupt the formation of the tubes, indicated by the *arrows*. At high concentrations (1,000 ng/ml; Fig. 6, *right column*), both endostatin and G129R-endostatin treatments eliminated the tubal structures, and the cells appeared to be dying. G129R treatment, serving as a negative control in this experiment, had no obvious effects on endothelial tube formation.

Pharmacokinetic Comparison of G129R, Endostatin, and G129R-Endostatin Fusion Protein. It has been demonstrated that increasing the size of a protein may increase its half-life (29). The relatively short serum half-life of G129R and endostatin present a considerable challenge to the clinical use of these potential therapeutic agents. To examine whether the pharmacokinetics of G129R-endosta-

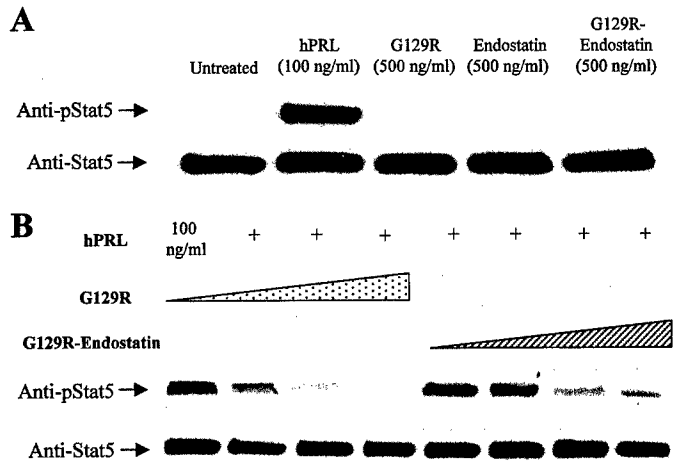

Fig. 4. Inhibition of STAT-5 phosphorylation by G129R-endostatin. T-47D human breast cancer cells were treated with the indicated amounts of PRL, G129R, and G129R-endostatin (*A*) or a dose-dependent combination treatment (*B*). Total protein was extracted and analyzed on a 4–15% gradient SDS-PAGE, followed by Western blotting with antiserum against either STAT-5-phosphorylated (*pStat5*) or STAT-5 as indicated in the appropriate panel. *A*, inhibition or stimulation of STAT5 phosphorylation of T-47D cells by PRL, G129R, endostatin, and G129R-endostatin. *B*, dose-dependent competitive inhibition of STAT-5-phosphorylation by G129R-endostatin. T-47D cells were incubated with PRL and increasing concentrations of G129R or G129R-endostatin. STAT5 and phosphorylated-STAT5 were detected by Western blot analysis as described in the "Materials and Methods."

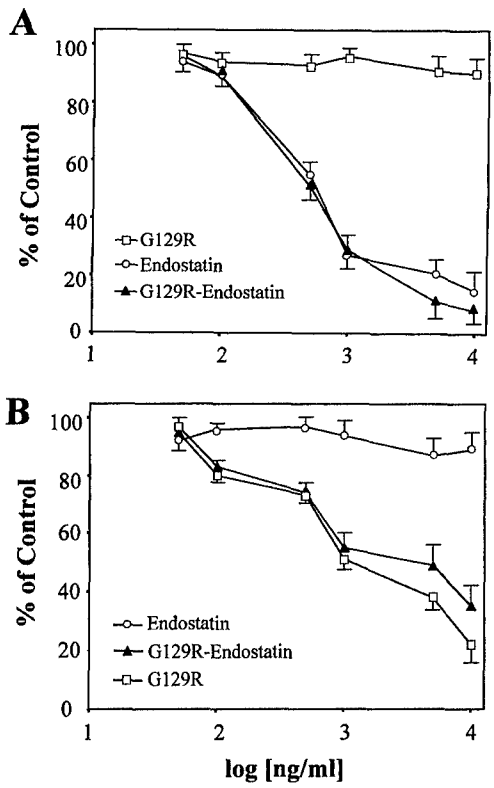

Fig. 5. Breast cancer and endothelial cell proliferation assay. Purified human endostatin, G129R-endostatin, and G129R were tested for their antiproliferative ability using HUVECs (*A*) and T-47D cells (*B*). Viability of cells was determined by the colorimetric MTS-PMS assay (Promega). Data are represented by the percentage of viable cells after treatments. *A*, ability of endostatin and G129R-endostatin to inhibit bFGF-induced endothelial cell proliferation using G129R as the control. *B*, effects of G129R and G129R-endostatin to inhibit the proliferation of human breast cancer cell line T-47D using endostatin as the control. Each experiment was carried out in triplicate, and the data are represented as the mean ± SE of three experiments.

tin were improved compared with G129R or endostatin alone, the *AUC* values of G129R, G129R-endostatin and endostatin were determined and compared after single i.p. injection (Fig. 7). The *AUC* was calculated for 200 μg of each protein based on the plot in Fig. 7. The *AUC* of G129R-endostatin is 7.3 times that of G129R and ~10 times that of endostatin. In addition, if taking into consideration the relative molar amounts of each protein injected (4.8 nmol of G129R-endostatin, as compared with 8.7 nmol of G129R or 10 nmol of endostatin was used in each experiment), the effective serum concentration of G129R-endostatin was found to be 13 times that of G129R and 21 times of equimolar amounts of endostatin. Thus, G129R-endostatin exhibits a higher effective serum concentration (and thus a longer serum half-life) than do G129R and endostatin.

G129R-Endostatin Fusion Protein Inhibits the Growth Rate of Breast Cancer Xenografts in Nude Mice. To test the efficacy of G129R-endostatin in inhibiting breast cancer, we used an aggressive murine breast cancer cell line, 4T1, in a nude mouse model. Fifty female athymic nude mice that were given injections of 4T1 cells (5×10^4) s.c. into the mammary fat pad were randomly divided into five groups. Postinoculation starting on day 5, G129R, endostatin, G129R-endostatin, and a combination treatment of G129R and endostatin were administered daily (i.p.). The control group was treated with 100 μl of PBS. Compared with control mouse group, all four of the treatments caused a significant reduction in tumor volume ($P < 0.0001$). Among the four treatment groups, G129R-endostatin (807 ± 235 mm^3) demonstrated the best inhibitory effects on 4T1 tumor growth and exhibited a statistically significant decrease in final tumor volume, compared with the control (2851 ± 305 mm^3; $P < 0.001$), G129R (1897 ± 194 mm^3; $P < 0.001$), endostatin (1271 ± 142 mm^3; $P < 0.001$), and the combination treatment (1399 ± 147 mm^3; $P = 0.0016$) groups (Fig. 8*A*). Similarly, all of the treatments caused significant reduction in the final tumor weights compared with the control group (1970 ± 410 mg): G129R-endostatin (841 ± 121 mg; $P < 0.001$); G129R (1409 ± 265 mg; $P < 0.001$), endostatin (1159 ± 170 mg; $P < 0.01$), and the combination of G129R and endostatin (1149 ± 195 mg; $P < 0.001$; Fig. 8*B*). G129R-endostatin treatment resulted in lower tumor weights than the other treatments in general. However, although this decrease was statistically significant compared with G129R ($P = 0.0004$), it was not significantly greater than that brought about by endostatin ($P = 0.0936$) or endostatin and G129R in combination ($P = 0.1065$).

DISCUSSION

Angiogenesis is the process of growth of new capillaries from preexisting blood vessels and is a crucial element for tumor sustenance (13). The switch of angiogenic phenotype in a tissue is dependent on the local balance between angiogenic factors and inhibitors (17). Of the many angiogenesis inhibitors that have been investigated and considered for potential cancer therapy, endostatin is one of the most potent and shows promise in inhibiting tumor growth in animals and in clinical trials (19).

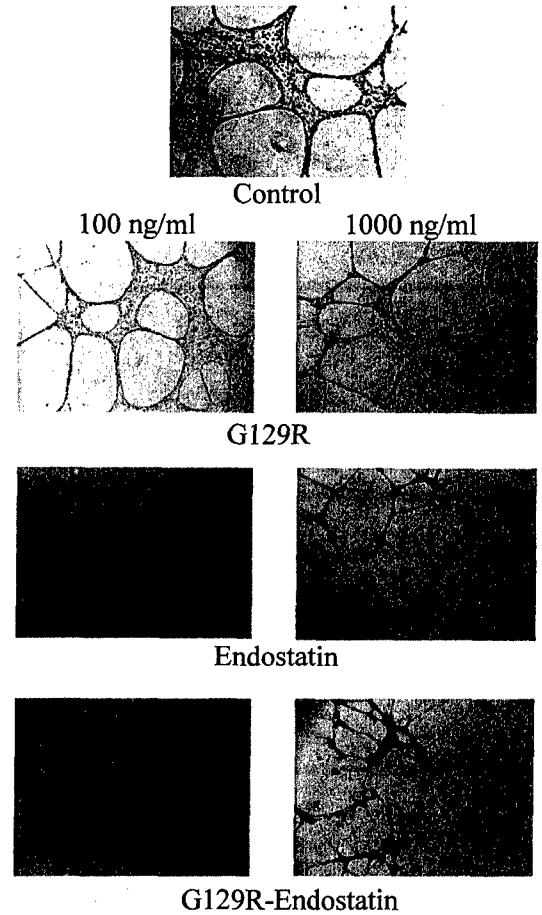

Fig. 6. The effect of G129R-endostatin on the three-dimensional structure of endothelial tubes. HUVECs (25,000 cells/well) in EGM-2 medium without antibiotic were plated onto Matrigel basement membrane-coated wells and were evaluated for their ability to form tubal structures similar to that of blood vessels. A low (100 ng/ml) and high (1000 ng/ml) concentration was used for endostatin, G129R-endostatin, and G129R. Each treatment was performed in triplicate. Untreated (*Control*) cells were processed similar to cells receiving drug treatment. Cells were viewed with a microscope and pictures were taken at ×10.

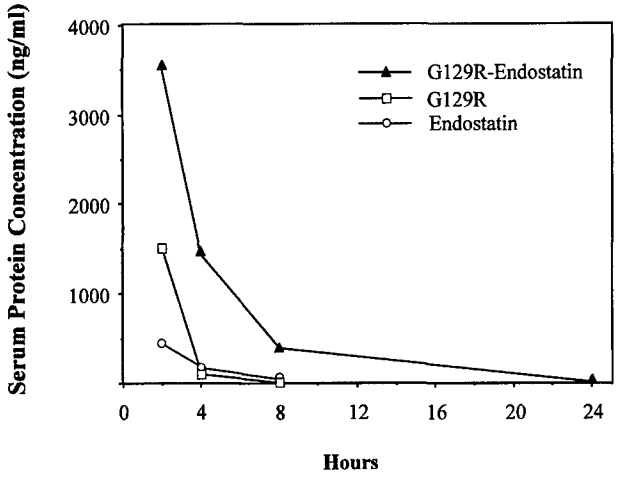

Fig. 7. Pharmacokinetic analysis of G129R-endostatin in BALB/c mice. Female BALB/c mice (n = 4) were given i.p. injections of G129R-endostatin (200 μg), G129R (200 μg), or endostatin (200 μg) and serum samples were collected by tail vein bleeding at the indicated time intervals. The serum concentration of G129R and G129R-endostatin was determined using the hPRL IRMA kit (DPC, Inc.). The serum concentration of endostatin was determined using the Accucyte ELISA protocol (Oncogene). The area under the curve (*AUC*) was determined for each protein. The *AUC* of G129R-endostatin is 7.3 times that of G129R. When adjusted for the relative molar amounts of each protein injected, the effective serum concentration of G129R-endostatin was found to be 13.1 times that of G129R for equimolar amounts of protein. The *AUC* for G129R-endostatin was 10-fold greater than the *AUC* for endostatin; this value was 21 for equimolar amounts of protein.

The underlying molecular mechanisms of antiangiogenic activity of endostatin are not fully understood, although several recent studies have begun to shed light on the mode of action of endostatin. Endostatin induces apoptosis causing G_1 arrest of endothelial cells through the inhibition of cyclin D1 (30) and may interrupt the Wnt signaling pathway, which is involved in cellular development (31). There is evidence that endostatin blocks the binding of vascular endothelial growth factor to endothelial cells (32) and inhibits the activation and catalytic activity of matrix metalloproteinases (33). Taken together, these studies suggest that the antitumor effects of endostatin are attributable to its specificity for endothelial cell proliferation rather than the direct inhibition of tumor cell growth (19). Successful attempts have been made to target endostatin to cancers of the breast and other tissues. For example, liposomes complexed with plasmids that encode endostatin inhibit breast tumor growth in mice when injected directly into tumors (34). Adenovirus-mediated systemic gene transfer of endostatin demonstrated significant reduction of tumor growth and inhibition of micrometastases in a mouse model (35). Together, these studies indicate that targeting endostatin directly to the tumor mass may improve the chance of tumor regression.

In view of the important role that PRL plays in breast cancer cell survival, the PRL antagonist, G129R, has demonstrated great potential as an antitumor agent. G129R inhibits breast cancer cell proliferation through the induction of apoptosis (10), in part, through the inhibition of *bcl-2* gene expression (13). Furthermore, G129R inhibits the growth of both T-47D and MCF-7 human breast cancer xenografts in nude mice (11). We have taken advantage of the ability of G129R to bind PRLR by designing targeted antitumor therapeutic agents. In this study, we genetically combined two proven effective anticancer agents that act via different mechanisms to create a novel bifunctional fusion protein, G129R-endostatin. We reasoned that a fusion protein consisting of G129R and endostatin would be targeted to breast cancer cells, inhibit tumor cell proliferation, and inhibit angiogenesis, which is required for proper development of the vascular network at the tumor site.

For endostatin to exert its antiangiogenic effects on the breast tumor microenvironment, both the G129R and the endostatin domains of G129R-endostatin fusion protein must recognize and bind receptors on breast cancer cells and endothelial cells, respectively. The specific binding of G129R-endostatin to the PRLR on breast cancer cells and to HUVECs was demonstrated by a radioreceptor binding assay and immunofluorescence/confocal microscopy. The binding affinity of G129R-endostatin to PRLR was similar to that of PRL and G129R. Thus, each portion of the fusion retained the ability to recognize its cognate receptor. The dual binding ability of the fusion protein was illustrated by dual immunofluorescence staining of both G129R and endostatin portions of G129R-endostatin. The binding pattern of endostatin to what appears to be the ECM in cultures of T-47D cells is interesting. The precise receptors/ligands to which endostatin binds have not been fully determined, and it is possible that, in the absence of preferred cell surface receptors on T-47D cells, endostatin associates with one or more ECM proteins. Because G129R itself has a high affinity for T-47D breast cancer cells, the G129R-endostatin fusion protein binds preferentially to these cells. Although the fusion protein binds to both breast cancer cells (T-47D) and endothelial cells via the appropriate domains, the individual domains of the fusion protein may not necessarily exhibit similar affinities for their respective ligands; the affinity of G129R for the PRLR may be greater than that of endostatin for its ligand(s) in the ECM. This may prove to be important in future clinical applications in which preferential localization

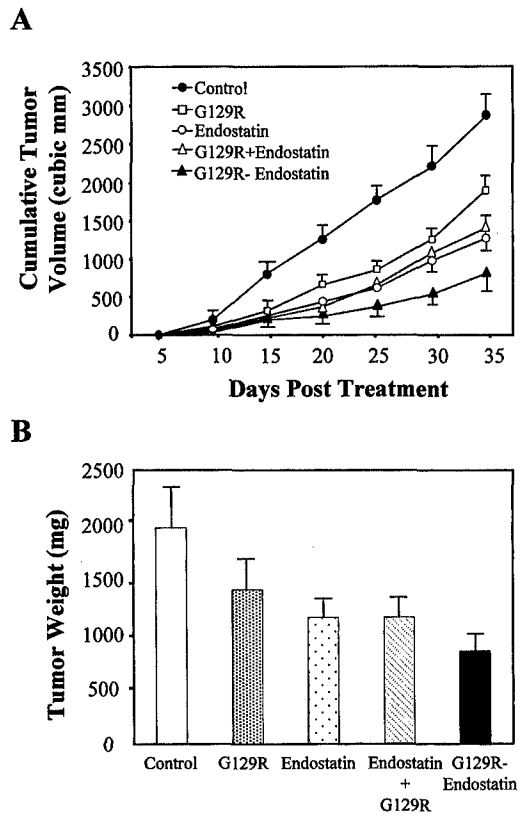

Fig. 8. *In vivo* analysis of human breast cancer inhibition using G129R-endostatin. Fifty athymic nude mice per group were inoculated (s.c.) with 5 × 10^4 4T1 cells. Tumors were allowed to establish for 5 days. Mice were randomized into five groups of 10 and were given injections of G129R (2.5 mg/kg/mouse), endostatin (2.5 mg/kg/mouse), G129R-endostatin (5 mg/kg/mouse), the combination of G129R (2.5 mg/kg/mouse) and endostatin (2.5 mg/kg/mouse), or 100 μl of sterile PBS for 35 consecutive days. *A*, tumor volume was determined every 5 days posttreatment by measuring the short axis (S) and the long axis (L) of the tumors and was calculated using the equation: $[S^2 \times L]/2$. Treatments of G129R-endostatin, G129R, endostatin, and G129R and endostatin in combination caused significant tumor reduction compared with the control group ($P < 0.005$). *B*, once the final tumor volume was measured, the tumors were removed and weighed. Values are represented as mean ± SE for each group (n = 10). All of the treatments caused significant reduction in the final tumor weights compared with the control group: G129R-endostatin ($P < 0.001$); G129R ($P < 0.001$), endostatin ($P < 0.01$), and the combination of G129R and endostatin ($P < 0.001$; *B*). In addition, G129R-endostatin-induced decrease in tumor weight was significantly greater than in G129R-treated mice ($P = 0.0004$), but not the endostatin ($P = 0.0936$) or endostatin and G129R combination ($P = 0.1065$) groups.

of G129R-endostatin to breast tumor tissue, instead of to vascular tissue in general, is essential.

Drug efficacy is, in part, affected by its serum half-life, a property that can be improved by increasing the size of a given molecule or protein (36). A potential limitation of the use of G129R and endostatin in cancer treatment is their relatively short serum-half-lives (29). One incentive to generate G129R-based fusion proteins for cancer therapy was to increase the serum half-life of G129R by increasing its size, a strategy that we used to generate a G129R fusion with interleukin 2 (G129R-interleukin 2; 29). In previous studies, G129R inhibited breast cancer xenografts at a dose of 5 mg (220 nmol)/kg/day (11), whereas inhibition of tumor growth, and an increase in serum half-life could be achieved by increasing endostatin to 20 mg (1 μmol)/kg/day (19, 21). The serum half-life of endostatin in mice has been found to be ~5 h (37). We have increased the serum half-life of G129R by mixing it with Matrigel or incorporating it into slow-releasing pellets (11), however, these methods currently are unsuitable for clinical studies. In this study, we demonstrate that one advantage of generating novel fusion proteins as therapeutics is that, along with the increased molecular size of the fusion protein, their serum half-lives are usually greatly extended. The effective serum concentration of G129R-endostatin is maintained over 24 h as shown in Fig. 7; this is significantly longer than that of either endostatin or G129R. We believe that this feature should contribute significantly in enhancing the antitumor effects of G129R-endostatin, especially in a clinical setting.

In summary, we have created a novel fusion protein, G129R-endostatin, consisting of the PRL antagonist G129R and the antiangiogenic protein endostatin. The fusion protein is a bifunctional protein that exhibits characteristics of G129R (the inhibition of breast cancer cell proliferation) and endostatin (inhibition of endothelial cell proliferation and development). More importantly, G129R-endostatin inhibits tumor growth at a dose much lower (5 mg/kg/day) than that reported for previous endostatin treatments (20 mg/kg/day). Given its bifunctional nature, G129R-endostatin, could become a potential therapeutic agent for the treatment of human breast cancer. Additional studies of the *in vivo* efficacy of G129R-endostatin will support its potential benefit in clinical application. The shortcomings of endostatin Phase II/III clinical trials may be ameliorated by a strategy, as described here, which increases the effective serum concentration of endostatin and targets it directly to the tumor site.

ACKNOWLEDGMENTS

We thank Jang Pyo Park, Susan Peirce, John Langenheim, Michele Scotti, and Dr. Thomas Wagner for their contributions to this project. We would also like to thank Eric Holle and Debra Cooper for their outstanding technical support for the mouse studies. Our appreciation goes to Brenda Welter and Dr. Lesly A. Temesvari for sharing their expertise in confocal microscopy.

REFERENCES

1. Blackwell, R. E., and Hammond, K. R. Hormonal control of normal breast morphology and function. *In:* A. Manni (ed.), Endocrinology of Breast Cancer, pp. 3–20. New Jersey: Humana Press, 1999.
2. Clevenger, C. V., Chang, W. P., Ngo, W., Pashe, T. L. M., Montone, K. T., and Tomaszewski, J. E. Expression of prolactin and prolactin receptor in human breast carcinoma. Evidence for an autocrine/paracrine loop. Am. J. Pathol., *146:* 695–705, 1995.
3. Nagasawa, H., Miura, K., Niki, K., and Namiki, H. Interrelationship between prolactin and progesterone in normal mammary gland growth in SHN virgin mice. Exp. Clin. Endocrinol., *86:* 357–360, 1985.
4. Vonderhaar, B. K. Prolactin: the forgotten hormone of human breast cancer. Pharmacol. Ther., *79:* 169–178, 1998.
5. Goffin, V., Kinet, S., Ferrag, F., Binart, N., Martial, J. A., and Kelly, P. A. Antagonistic properties of human prolactin analogs that show paradoxical agonistic activity in the Nb2 bioassay. J. Biol. Chem., *271:* 16573–16579, 1996.
6. Goffin, V., and Kelly, P. A. The prolactin/growth hormone receptor family: structure/function relationships. J. Mammary Gland Biol. Neoplasia, *2:* 7–17, 1997.
7. Vonderhaar, B. K. Prolactin involvement in breast cancer. Endocr.-Related Cancer, *6:* 389–404, 1999.
8. Kelly, P. A., Djiane, J., Postel-Vinay, M. C., and Edery, M. The prolactin/growth hormone receptor family. Endocr. Rev., *12:* 235–251, 1991.
9. Cecim, M., Fadden, C., Kerr, J., Steger, R. W., and Bartke, A. Infertility in transgenic mice over expressing the bovine growth hormone gene: disruption of the neuroendocrine control of prolactin secretion during pregnancy. Biol. Reprod., *52:* 1187–1192, 1995.
10. Chen, W. Y., Ramamoorthy, P., Chen, N., Sticca, R., and Wagner, T. E. A human prolactin antagonist, hPRL-G129R, inhibits breast cancer cell proliferation through induction of apoptosis. Clin. Cancer Res., *5:* 3583–3593, 1999.
11. Chen, N. Y., Holle, L., Li, W., Peirce, S. K., Beck, M. T., and Chen, W. Y. *In vivo* studies of the anti-tumor effects of a human prolactin antagonist, hPRL-G129R. Int. J. Oncol., *20:* 813–818, 2002.
12. Cataldo, L., Chen, N. Y., Yuan, Q., Li, W., Ramamoorthy, P., Wagner, T. E., Sticca, R. P., and Chen, W. Y. Inhibition of oncogene *STAT3* phosphorylation by a prolactin antagonist, hPRL-G129R, in T-47D human breast cancer cells. Int. J. Oncol., *17:* 1179–1185, 2000.
13. Beck, M. T., Peirce, S. K., Chen, W. Y. Regulation of *bcl-2* gene expression in human breast cancer cells by prolactin and its antagonist, hPRL-G129R. Oncogene, *21:* 5047–5055, 2002.
14. Folkman, J. Tumor angiogenesis. Adv. Cancer Res., *19:* 331–358, 1974.
15. Kirsch, M., Schackert, G., and Black, P. M. Angiogenesis, metastasis, and endogenous inhibition. J. Neurooncol., *50:* 173–180, 2000.
16. Saaristo, A., Karpanen, T., and Alitalo, K. Mechanisms of angiogenesis inhibitors and their use in the inhibition of tumor growth and metastasis. Oncogene, *19:* 6122–6129, 2000.
17. Rastinejad, F., Polverini, P. J., and Bouck, N. P. Regulation of the activity of a new inhibitor of angiogenesis by a cancer suppressor gene. Cell, *56:* 345–355, 1989.
18. Folkman, J. Tumor angiogenesis: therapeutic implications. N. Engl. J. Med., *285:* 1182–1186, 1971.
19. Ryan, C. J., and Wilding, G. Angiogenesis inhibitors. New agents in cancer therapy. Drugs Aging, *17:* 249–255, 2000.
20. Sim, B. K., MacDonald, N. J., and Gubish, E. R. Angiostatin and endostatin: endogenous inhibitors of tumor growth. Cancer Metastasis Rev., *19:* 181–190, 2000.
21. O'Reilly, M. S., Boehm, T., Shing, Y., Fukai, N., Vasios, G., Lane, W. S., Flynn, E., Birkhead, J. R., Olsen, B. R., and Folkman, J. Endostatin: an endogenous inhibitor of angiogenesis and tumor growth. Cell, *88:* 277–285, 1997.
22. Standker, L., Schrader, M., Kanse, S. M., Jurgens, M., Forssmann, W. G., and Preissner, K. T. Isolation and characterization of the circulating form of human endostatin. FEBS Lett., *420:* 129–133, 1997.
23. Taddei, L., Chiarugi, P., Brogelli, L., Cirri, P., Magnelli, L., Raugei, G., Ziche, M., Granger, H. J., Chiarugi, V., and Ramponi, G. Inhibitory effect of full-length human endostatin on *in vitro* angiogenesis. Biochem. Biophys. Res. Commun., *24:* 340–345, 1999.
24. Dhanabal, M., Ramchandran, R., Waterman, M. J., Lu, H., Knebelmann, B., Segal, M., and Sukhatme, V. P. Endostatin induces endothelial cell apoptosis. J. Biol. Chem., *274:* 11721–11726, 1999.
25. Yokoyama, Y., Green, J. E., Sukhatme, V. P., and Ramakrishnan, S. Effect of endostatin on spontaneous tumorigenesis of mammary adenocarcinoma in a transgenic mouse model. Cancer Res., *60:* 4362–4365, 2000.
26. Sasaki, T., Larsson, H., Kreuger, J., Salmivirta, M., Claesson-Welsh, L., Lindahl, U., Hohenester, E., and Timpel, R. Structural basis and potential role of heparin/heparan sulfate binding to the angiogenesis inhibitor endostatin. EMBO J., *18:* 6240–6248, 1999.
27. Boehm, T., Folkman, J., Browder, T., and O'Reilly. M. S. Antiangiogenic therapy of experimental cancer does not induce acquired drug resistance. Nature (Lond.), *390:* 404–407, 1997.
28. Huang, X., Wong, M. K., Zhao, Q., Zhu, Z., Wang, K. Z., Huang, N., Ye, C., Gorelik, E., and Li, M. Soluble recombinant endostatin purified from *Escherichia coli*: antiangiogenic activity and antitumor effect. Cancer Res., *61:* 478–481, 2002.
29. Zhang, G., Li, W., Holle, L., Chen, N., Chen, W. Y. A. novel design of targeted endocrine and cytokine therapy for breast cancer. Clin. Cancer Res., *8:* 1196–1205, 2002.
30. Hanai, J., Dhanabal, M., Karumanchi, S. A., Albanese, C., Waterman, M., Chan, B., Ramchandran, R., Pestell, R., and Sukhatme, V. P. Endostatin causes G_1 arrest of endothelial cells through inhibition of cyclin. J. Biol. Chem., *277:* 16464–16469, 2002.
31. Hanai, J., Gloy, J., Karumanchi, S. A., Kale, S., Tang, J., Hu, G., Chan, B., Ramchandran, R., Jha, V., Sukhatme, V. P., and Sokol, S. Endostatin is a potential inhibitor of Wnt signaling. J. Cell Biol., *158:* 529- 539, 2002.
32. Kim, Y. M., Hwang, S., Kim, Y. M., Pyun, B. J., Kim, T. Y., Lee, S. T., Gho, Y. S., and Kwon, Y. G. Endostatin blocks vascular endothelial growth factor-mediated signaling via direct interaction with KDR/Flk-1. J. Biol. Chem., *277:* 27872–27879, 2002.
33. Kim, Y. M., Jang, J. W., Lee, O. H., Yeon, J., Choi, E. Y., Kim, K. W., Lee, S. T., and Kwon, Y. G. Endostatin inhibits endothelial and tumor cellular invasion by blocking the activation and catalytic activity of matrix metalloproteinase. Cancer Res., *60:* 5410–5413, 2000.
34. Sacco, M. G., Cato, E. M., Ceruti, R., Soldati, S., Indraccolo, S., Caniatti, M., Scanziani, E., and Vezzoni, P. Systemic gene therapy with anti-angiogenic factors inhibits spontaneous breast tumor growth and metastasis in MMTVneu transgenic mice. Gene Ther., *8:* 67–70, 2001.
35. Sauter, B. V., Martinet, O., Zhang, W. J., Mandeli, J., and Woo, S. L. Adenovirus-mediated gene transfer of endostatin *in vivo* results in high level of transgene expression and inhibition of tumor growth and metastases. Proc. Natl. Acad. Sci. USA, *97:* 4802–4807, 2000.
36. Dennis, M. S., Zhang, M., Meng, Y. G., Kadkhodayan, M., Kirchhofer, D., Combs, D., and Damico, L. A. Albumin binding as a general strategy for improving the pharmacokinetics of proteins. J. Biol. Chem., *277:* 35035–35043, 2002.
37. Sim, B. K. L., Folger, W. E., Zhou, X. H., Liang, H., Madsen, J. W., Luu, K., O'Reilly, M. S., Tomaszewski, J. E., and Fortier, A. H. Zinc ligand-disrupted recombinant human endostatin: potent inhibition of tumor growth, safety and pharmacokinetic profile. Angiogenesis, *3:* 41–51, 1999.